High-throughput transposon sequencing highlights the cell wall as an important barrier for osmotic stress in methicillin resistant *Staphylococcus aureus* and underlines a tailored response to different osmotic stressors

Short Title: Global analysis of osmotic stress responses in Staphylococcus aureus

Christopher F. Schuster[a], David M. Wiedemann[a], Freja C. M. Kirsebom[a,1], Marina Santiago[b], Suzanne Walker[b] and Angelika Gründling[a,2]

ORCID IDs: 0000-0002-4566-7226 (CFS), 0000-0001-6961-0980 (DMW), 0000-0003-4585-319X (FCK), 0000-0002-5446-3452 (MS), 0000-0002-0545-914X (SW), 0000-0002-6235-8687 (AG)

[a]Section of Molecular Microbiology and MRC Centre for Molecular Bacteriology and Infection, Imperial College London, London, SW7 2AZ, U.K.

[b]Department of Microbiology and Immunobiology, Harvard Medical School, Boston, MA 02115, U.S.A.

[1]Current address: Section of Respiratory Infections, National Heart and Lung Institute, Imperial College London, London, W2 1PG, U.K.

[2]To whom correspondence should be addressed. Email: a.grundling@imperial.ac.uk, Phone: 0044 20 7594 5256

Keywords: osmotic stress, NaCl, KCl, Sucrose, *S. aureus*, DUF25380, PBP2

Summary

Staphylococcus aureus is an opportunistic pathogen that can cause soft tissue infections but is also a frequent cause of foodborne illnesses. One contributing factor for this food association is its high salt tolerance allowing this organism to survive commonly used food preservation methods. How this resistance is mediated is poorly understood, particularly during long-term exposure. In this study, we used TN-seq to understand how the responses to osmotic stressors differ. Our results revealed distinctly different long-term responses to NaCl, KCl and sucrose stresses. In addition, we identified the DUF2538 domain containing gene *SAUSA300_0957* (gene *957*) as essential under salt stress. Interestingly, a *957* mutant was less susceptible to oxacillin and showed increased peptidoglycan crosslinking. The salt sensitivity phenotype could be suppressed by amino acid substitutions in the transglycosylase domain of the penicillin binding protein Pbp2, and these changes restored the peptidoglycan crosslinking to WT levels. These results indicate that increased crosslinking of the peptidoglycan polymer can be detrimental and highlight a critical role of the bacterial cell wall for osmotic stress resistance. This study will serve as a starting point for future research on osmotic stress response and help develop better strategies to tackle foodborne staphylococcal infections.

Introduction

Staphylococcus aureus is a Gram-positive bacterium that is carried by about 20 % of healthy individuals (Wertheim *et al.*, 2005). It is also an opportunistic pathogen causing a variety of diseases, including bacteremia, endocarditis, soft tissue infections and food poisoning (Tong *et al.*, 2015). One characteristic of *S. aureus* is its ability to grow in the presence of a high salt concentration (up to 2.5 M). Many other bacteria are unable to grow under these conditions

24 (Measures, 1975), and this has been used extensively for the isolation of staphylococci. This salt
25 tolerance also allows *S. aureus* to thrive in its niches such as the human nares, skin (Wertheim *et*
26 *al.*, 2005) and certain food products (Adams & Moss, 2008).

27 Bacterial cells are highly pressurized (up to 1.9 MPa for *Bacillus subtilis* (Whatmore & Reed,
28 1990)) and contain a strongly crowded cytoplasm that is hyperosmotic to the environment. Water
29 is not transported into the cell actively but rather influxes passively into the cell due to the high
30 internal osmolality. Whenever the extracellular osmolality increases, water exits the cell which can
31 cause problems to multiple cellular processes, in part due to molecular crowding (Wood, 2011,
32 van den Berg *et al.*, 2017). Hence, *S. aureus* must possess strategies to counter the effects of salt
33 damage, but these are not entirely understood, as most work has been performed in *Escherichia*
34 *coli* and *B. subtilis*.

35 General mechanisms of hyper-osmotic stress mitigation in bacteria are the rapid import of
36 potassium and the accumulation of small osmotically active compounds, named compatible
37 solutes (reviewed in depth by (Bremer & Krämer, 2019, Gunde-Cimerman *et al.*, 2018, Booth,
38 2014, Cox *et al.*, 2018)). Potassium levels quickly subside in favor of an increase in the
39 concentration of compatible solutes.

40 In *S. aureus,* results consistent with the uptake of potassium (Csonka, 1989, Csonka & Hanson,
41 1991, Sleator & Hill, 2002) followed by the accumulation of compatible solutes have been
42 reported (Measures, 1975, Graham & Wilkinson, 1992, Christian & Waltho, 1964). The most
43 effective compatible solutes in *S. aureus* are glycine betaine and proline (Miller *et al.*, 1991,
44 Measures, 1975, Townsend & Wilkinson, 1992, Anderson & Witter, 1982, Bae & Miller, 1992,
45 Pourkomailian & Booth, 1992), which are imported by specific osmolyte transporters (Bae &
46 Miller, 1992, Pourkomailian & Booth, 1992). These preferred osmolytes can accumulate in the cell
47 to very high concentrations without negatively affecting cellular processes (Csonka & Hanson,
48 1991). In addition, *S. aureus* can also synthesize compatible solutes *de novo*, as in the case of

49 glutamine (Anderson & Witter, 1982), but this process is much slower than the uptake of
50 osmolytes and requires more energy.

51 Previous research investigating the underlying genetic factors of the *S. aureus* osmotic stress
52 response implicated several osmolyte transporters in this process (Price-Whelan *et al.*, 2013,
53 Scybert *et al.*, 2003, Schwan *et al.*, 2006, Vijaranakul *et al.*, 1998, Wengender & Miller, 1995).
54 These include the potassium transport systems Kdp and Ktr (Price-Whelan *et al.*, 2013), the proline
55 transporter PutP (Wengender & Miller, 1995, Schwan *et al.*, 2006), the arsenic transport system
56 Ars (Scybert *et al.*, 2003) and the branched chain amino acid uptake system BrnQ (Vijaranakul *et*
57 *al.*, 1998). In addition, although currently not experimentally verified in *S. aureus*, it can be
58 assumed that the main glycine betaine uptake system OpuD (Wetzel *et al.*, 2011, Zeden *et al.*,
59 2018) is an important factor in *S. aureus* for osmotic adaptation as glycine betaine uptake reduces
60 sensitivity to NaCl exposure (Miller *et al.*, 1991). Of note, in recent time the second messenger
61 cyclic-dinucleotide-AMP (c-di-AMP) (Corrigan & Gründling, 2013) has been tied to the regulation
62 of osmotic stress in *S. aureus* and other Gram-positive bacteria (reviewed by Commichau *et al.*,
63 2018). This is through the interaction and regulation of a number of potassium (Corrigan *et al.*,
64 2013) and compatible solute transporters by c-di-AMP (Schuster *et al.*, 2016).

65 Despite these multiple countermeasures, exposure of *S. aureus* to osmotic stress leads to
66 morphological changes, including the formation of larger cells (Vijaranakul *et al.*, 1995) and a
67 thickening of the cell wall (Onyango *et al.*, 2013). However, if and which genetic factors are
68 required for those processes are currently not well understood. The cell wall of Gram-positive
69 bacteria is an important barrier and acts as a counterpart to the pressurized cytoplasm. A major
70 component of the cell wall is peptidoglycan, a polymer consisting of chains of repeating N-
71 acetylglucosamine (GlcNAc) and N-acetylmuramic acid (MurNAc) units that are crosslinked with
72 neighboring chains via short peptides and, in the case of *S. aureus,* pentaglycine cross-bridges
73 (Reviewed by (Vollmer *et al.*, 2008)). In the past, the contribution of the cell wall towards osmotic

74 stress resistance was often not considered in the bacterial osmotic stress resistance field. Partly,
75 because the integrity of the cell wall is often assumed to be a prerequisite rather than an active
76 adaptation to survive osmotic stresses and partly because most cell envelope stress sensing
77 systems are unable to directly sense osmotic stresses (Jordan *et al.*, 2008).

78 Nevertheless, several possible changes to the cell wall have been observed *in S. aureus* during
79 NaCl stress, such as shortened interpeptide bridges in the peptidoglycan (Vijaranakul *et al.*, 1995),
80 an increase in resistance to methicillin (Madiraju *et al.*, 1987) and increased autolysis activity
81 (Stapleton *et al.*, 2007, Ochiai, 2000). In addition to peptidoglycan, other components within the
82 cell envelope, such as teichoic acids and more specifically their modifications with D-alanine
83 (Koprivnjak *et al.*, 2006) and sugar residues (Mistretta *et al.*, 2019, Kho & Meredith, 2018) are
84 affected by osmotic stress. Combined, these findings indicate that the integrity of the cell wall is
85 an important requirement for osmotic resistance.

86 Most studies on osmotic stress in *S. aureus* have been conducted using NaCl salt as the
87 osmotic stressor. The ionic properties of NaCl have important implications on protein stability and
88 activity as its accumulation can lead to denaturation of proteins. A few studies in *S. aureus* have
89 also been performed with non-ionic osmotic stressors such as sucrose, sorbitol glycerol and amino
90 acids (Stewart *et al.*, 2005, Stewart *et al.*, 2002, Mitchell & Moyle, 1959, Schwan *et al.*, 2006). All
91 of these different stresses are often used synonymously with osmotic stress, in part influenced by
92 the findings that the initial mitigation of osmotic stress by either salts or sugars can be prevented
93 by the accumulation of potassium and compatible solutes. However, there are potential
94 differences in the long-term adaptation to ionic and non-ionic osmotic stressors, which up to date
95 have not been investigated in detail. It is currently also not known if the adaptations besides the
96 accumulation of potassium and osmolytes are similar or differ depending on the osmotic stressor,
97 and this was addressed as part of this study.

98

99 Using a transposon insertion sequencing (TN-seq) method (Santiago *et al.*, 2015), we
100 determined on a whole genome level genes that are essential or dispensable during long-term
101 osmotic stress caused by exposure to NaCl, KCl and sucrose. This yielded very different sets of
102 essential and dispensable candidate genes, providing experimental evidence of the distinct nature
103 of these stresses and linking a number of previously unknown factors to the osmotic stress
104 response in *S. aureus*. Amongst other novel candidate genes, we identified gene *SAUSA300_0957*
105 as an important NaCl resistance gene in *S. aureus* and show that the encoded protein is important
106 for peptidoglycan homeostasis in *S. aureus*. Another protein, which we identified as important
107 during salt stress, is the penicillin binding protein Pbp2, further emphasizing a key function of
108 peptidoglycan during NaCl-induced osmotic stress. Taken together, these experiments highlight
109 the bacterial cell wall as a key player in the salt stress response of *S. aureus*.

110 **Results**

111 **Different types of osmotic stresses target different sets of genes**

112 In the literature, osmotic stress is a loosely used term, however the type of ion or osmolyte can
113 potentially have a great impact on how bacteria respond. To address this issue, we determined
114 how the stress responses to different commonly used osmolytes compare. A highly saturated *S.*
115 *aureus* transposon library was generated with a promoter-less transposon (Santiago *et al.*, 2015)
116 and subsequently used for transposon sequencing (TN-seq) experiments (Supplementary Table 1
117 for details on all TN-seq experiments). The library was propagated for 16 generations in either LB
118 medium (Lennox) or in LB with extra 0.5 M NaCl, 0.5 M KCl or 1.0 M sucrose added (Fig. 1A). The
119 molarity of sucrose was doubled to accommodate for the dissociation of the salts into two ions
120 and hence leading to roughly the same osmolality. The culture challenged with 0.5 M NaCl grew
121 the slowest, followed by 1.0 M sucrose, whereas the cells grown in 0.5 M KCl grew similarly to the

122 cells grown in LB (Fig. 1B). As expected for a good quality transposon library, transposon insertions
123 were found under all conditions in genes throughout the whole genome (Fig. 1C). Next, the
124 number of TN-insertions per gene following growth under the NaCl, KCl or sucrose stress condition
125 was compared to the number of TN-insertions per gene after growth in LB medium
126 (Supplementary Table 2) and in this manner conditionally essential (Supplementary Table S3) and
127 dispensable (Supplementary Table S4) genes identified. Fold-changes in transposon insertions per
128 gene and q-values were plotted in volcano plots (Fig. 1D). From this, it was evident that under KCl
129 stress the number of essential and dispensable genes was much lower than for NaCl or sucrose
130 stress, indicating a much less severe effect of KCl on *S. aureus* cells. This was also reflected when
131 inspecting the gene lists of the top 30 essential or dispensable genes (Supplementary Table S3 and
132 S4) as in the KCl condition only 15 and 2 genes respectively met the requirements of q-value ≤ 0.05
133 and a fold-change of 5. To identify common genes between conditions, the fold-change stringency
134 was relaxed to 2-fold and the overlap of genes was visualized in Venn diagrams (Fig. 1E, individual
135 genes in Supplementary Table S5). Three genes, namely *SAUSA300_0425* (*USA300HOU_0457*,
136 *mpsA* (*nuoF*)) coding for a cation transporter of the respiratory chain (Mayer *et al.*, 2015),
137 *SAUSA300*_0750 (*USA300HOU_0796*, *whiA*) coding for a protein of unknown function and
138 SAUSA300_0846 (USA300HOU_0903) encoding a possible sodium:proton antiporter were
139 essential in all conditions. In the case of dispensable genes, only one gene, *SAUSA300_1255*
140 (*USA300HOU_1294*, *mprF/fmtC*), coding for a phosphatidylglycerol lysyltransferase involved in the
141 defense against cationic microbial peptides, was identified in all conditions (Fig. 1E,
142 Supplementary Table S5). To assess similarities and differences on a gene function and cellular
143 pathway level, functional Voronoi maps were generated from the conditionally essential
144 (Supplementary Fig. S1) and dispensable (Supplementary Fig. S2) genes regardless of their p-
145 values. These images highlighted the essentiality of the wall teichoic acid through *tagO* and the *dlt*
146 operon (Supplementary Fig. S1A) and the transporters AapA and MgtE in both NaCl

147 (Supplementary Fig. S1A) and KCl (Supplementary Fig. S1B) but not in the sucrose stress condition
148 (Supplementary Fig. S1C). When the dispensable genes were investigated (Supplementary Fig. S2),
149 the number and type of genes in the NaCl condition differed considerably from KCl and sucrose
150 stress. Under NaCl stress (Supplementary Fig. S2A), in addition to the penicillin binding protein
151 *pbp2*, a large number of genes involved in respiration were found to be dispensable
152 (Supplementary Fig. S2A). The number of dispensable genes in the KCl (Supplementary Fig. S2B)
153 and sucrose (Supplementary Fig. S2C) conditions were considerably lower. Taken together, the
154 overlaps between conditions were small, indicating distinct modes of actions for each osmotic
155 stress.
156

157 **TN-seq is a robust method to identify *S. aureus* genes involved in NaCl stress**

158 In our experiments, NaCl stress elicited the strongest response. We therefore focused our
159 further analysis on the *S. aureus* salt stress response and conducted two additional TN-seq screens
160 to confirm the robustness of this approach (Figure 2A). TN-seq screens were performed using a
161 previously published library (Santiago *et al.*, 2015, Coe *et al.*, 2019) with six transposon variants
162 and the library containing only one transposon variant used in the first TN-seq experiment
163 (Supplementary Table S1 for overview). The libraries were propagated for 17 generations in either
164 LB or in medium containing 0.5 M NaCl (Fig. 2B). When the libraries were grown in high salt
165 medium, clustering of transposon insertions in certain regions was observed due to the
166 enrichment of better salt-adapted TN-strains (Supplementary Fig. S3). The fold-changes of
167 transposon insertions per gene under the salt stress conditions compared to the LB condition
168 (input library) as well as q-values were determined for each gene (Supplementary Table S6-S7).
169 The data were plotted as volcano plots (Fig. 2C), revealing similar numbers of conditional salt
170 essential and dispensable genes in both replicates. A good overlap of the top essential and

171 dispensable genes was observed between the replicates, confirming the robustness of the TN-Seq
172 screens (Supplementary Tables S8-11).

173 **The TN-seq screens highlight the essentiality of transporters and cell envelope related genes and**
174 **the dispensability of respiration genes under high salt conditions**

175 In both replicates, genes coding for transporters and cell envelope related genes were the
176 most prominent conditionally salt essential genes (Voronoi maps in Supplementary Fig. S4-S5, Top
177 essential and dispensable genes in Supplementary Tables S8-S11). More specifically, the TN-seq
178 data indicated that inactivation of the putative magnesium transporter MgtE (Schuster *et al.*,
179 2019) and the putative D-serine/D-alanine/glycine transporter AapA is detrimental under salt
180 stress (Voronoi maps in Supplementary Fig. S4, Top essential genes in Supplementary Tables S8
181 and S10). In addition, the *dlt* operon, coding for enzymes required for the D-alanylation of teichoic
182 acids, an important factor for cationic peptide resistance (Brown *et al.*, 2013), as well as the
183 stationary and stress sigma factor gene *sigB* were found to be essential.

184 An even larger number of genes was identified as dispensable during salt stress (Voronoi
185 maps in Supplementary Fig. S5, Top dispensable genes in Supplementary Tables S9 and S11).
186 Inactivating or reducing the expression of such genes is expected to help *S. aureus* survive under
187 salt stress. Among these dispensable genes were genes coding for the sodium antiporter Mnh2,
188 which has previously been shown to transport Na^+/H^+ and K^+/H^+ in high pH medium and to play an
189 important role in cytoplasmic pH maintenance (Vaish *et al.*, 2018). As noted earlier, a large
190 number of genes involved in respiration, such as the *cta/qox/men/hem* genes as well as genes
191 involved indirectly in respiration through quinone synthesis (shikimate pathway, *aro* operon) were
192 also identified as dispensable during salt stress. The data also reproducibly indicated that genes
193 coding for the phosphodiesterases GdpP and Pde2 involved in degradation of the signaling
194 molecule c-di-AMP are dispensable under high salt conditions. Using the TN-seq approach, we

195 were able to identify a large number of *S. aureus* genes as potentially dispensable or essential
196 when this organism is exposed to high salt.

197 **Tn-seq reveals previously unidentified salt resistance genes during long-term salt exposure**

198 The TN-seq method relies on the enrichment of strains adapted to certain growth conditions
199 and is therefore ideal for exploring the long-term effects on growth in response to salt stress. In a
200 previous study (Price-Whelan *et al.*, 2013), the adaptation of *S. aureus* to 2 M NaCl stress after 6
201 generations of growth was determined on a transcriptome level. This work highlighted the
202 importance of K^+ transporters for *S. aureus* to survive a high salt exposure. To evaluate how our
203 results compare, we determined the overlaps between our datasets and the microarray data. To
204 this end, the *S. aureus* strain COL locus tags used in the microarray study were converted to
205 TCH1516 locus tags where possible (Supplementary Table S12) and compared to the two TN-seq
206 datasets. The overlap between the downregulated (microarray) and dispensable (TN-seq) genes
207 was minimal in both replicates (1 and 7) and also very small for the upregulated and essential
208 genes (both 14). Three operons were consistently essential or upregulated between all datasets:
209 the *cap5*, *SAUSA300_0771-2*, and the *sda* operon. The *cap5* genes are involved in capsule
210 production (Chan *et al.*, 2014) and have been previously reported to be induced by the addition of
211 salt (Pöhlmann-Dietze *et al.*, 2000). Genes *SAUSA300_0771-2* encode for membrane proteins that
212 are predicted to form a threonine/serine exporter (Interpro database IDs: IPR010619 and
213 IPR024528) and the *sda* genes are annotated as L-serine dehydratase components and a regulator
214 protein. The low overlap between the microarray and TN-seq data (Supplementary Table S12)
215 suggests that in our screen we have identified a number of previously unknown salt tolerance
216 genes.

217 **Confirmation of genes essential during salt stress using defined mutants**

218 To determine to what extent different genes identified in the TN-seq screen contribute to the
219 salt resistance of *S. aureus*, a set of potentially salt essential genes from dataset B were chosen for
220 further investigation (Supplementary Table S13). For this analysis we used defined transposon
221 mutants available from the *S. aureus* NTML transposon mutant library (Fey *et al.*, 2013). The
222 growth of the different NTML transposon mutant strains was assessed in LB and LB 0.5 M NaCl
223 medium. In LB medium, most strains grew similarly to the WT strain JE2, indicating that
224 inactivation of the respective gene does not greatly affect bacterial growth in normal LB medium
225 (Supplementary Figs. S6A-D, left panels). Exceptions were strains NE1109 (*sigB*), NE1778 (*lcpB*) and
226 NE188 (*mfd*), cultures of which reached slightly lower final optical densities (Supplementary Figs.
227 S6A-D, left panels). At high osmolality conditions (LB 0.5 M NaCl), all strains showed a growth
228 defect compared to the WT strain (Supplementary Figs. S6A-D, right panels), validating the TN-seq
229 as a method to identify *S. aureus* genes that are important during salt stress. Several strains
230 exhibited strong growth defects in the presence of 0.5 M NaCl with strain NE1384, containing a
231 transposon insertion in *SAUSA300_0957* showing extremely reduced growth (Supplementary Figs.
232 S6C and D). To confirm that the salt sensitivity was mediated by the inactivation of the genes in
233 questions, we constructed complementation plasmids for seven of the most promising candidates
234 by either expressing the gene of interest from its native promoter or an anhydrotetracycline (Atet)
235 inducible promoter in the transposon mutant strains. While no complementation was observed
236 for four strains (Supplementary Figs. S7A and S7B), the salt-dependent growth defect could be
237 complemented for strains carrying mutations in *SAUSA300_0694* (Fig. 3A), *SAUSA300_0910* (*mgtE*)
238 and *SAUSA300_0957* (Fig. 3B). *SAUSA300_0694* encodes a hypothetical protein with 6 predicted
239 transmembrane helices but no other identifiable domain motif. MgtE (SAUSA300_0910) is a
240 predicted magnesium transporter, which we have recently shown can also contribute to cobalt
241 toxicity in *S. aureus* (Schuster *et al.*, 2019). *SAUSA300_0957* (from here on out referred to as gene

242 *957*) codes for a cytoplasmic protein with a DUF2538 domain of unknown function that is
243 conserved in Actinobacteria and Firmicutes. We further investigated this gene in this study
244 because the *957* mutant exhibited the strongest salt-sensitivity phenotype (Fig. 3B).

245 **Deletion of gene *957* causes physiological changes leading to a smaller cell size**

246 As all previous experiments were performed with transposon mutants, we first constructed
247 strain LAC*Δ*957* with a marker-less in-frame deletion of gene *957*. Strain LAC*Δ*957* had the
248 expected growth defect in the presence of 0.5 M NaCl and this phenotype could be complemented
249 by expressing a functional copy of *957* (Fig. 4A). To gain further insight into the molecular function
250 of gene *957*, we analyzed the neighboring genomic area. Transcriptome data (Mäder *et al.*, 2016)
251 suggested that gene *957* is in an operon with *lcpB* (Fig. 4B), which is one of three wall teichoic acid
252 (WTA) ligases present in *S. aureus* (Chan *et al.*, 2013, Over *et al.*, 2011, Schaefer *et al.*, 2017). *fmtA*
253 is located upstream of *957* and has been proposed to code for an esterase that can remove D-
254 alanine modifications from teichoic acids (Rahman *et al.*, 2016) and is involved in methicillin
255 resistance (Berger-Bächi *et al.*, 1989). Genes coding for a predicted acetyltransferase and *atl*
256 coding for the major *S. aureus* autolysin are found immediately downstream of the *957* operon
257 (Oshida *et al.*, 1995). Due to the presence of many cell envelope related genes in the vicinity of
258 gene *957*, we proceeded to test if the *957* mutant displays other phenotypes connected to cell
259 envelope homeostasis. First, WT LAC*, the *957* mutant and the complementation strain were
260 grown in LB and the ratio of colony forming units to optical density (CFU/OD) was determined. The
261 CFU/OD ratio was significantly larger for the *957* mutant (60.8±6.8 x10^7 CFU/OD) mutant as
262 compared to strain LAC* (37.5±9.3 x10^7 CFU/OD) when grown in LB, suggesting a change in cell
263 shape or size (Fig. 4C). This phenotype was restored in the complementation strain (37.3±3.6 x10^7
264 CFU/OD) (Fig. 4C). When the average cell diameter was determined by microscopy, a small but
265 significant reduction in cell diameter was seen for the *957* mutant (1.25±0.02 µm) as compared to

266 the WT (1.36±0.03 µm) and the cell size was restored to wild type levels in the complementation
267 strain (1.35±0.05 nm) (Fig. 4D). These results support our hypothesis that the envelope might be a
268 target of *gene 957* and prompted us to look into these processes in more detail.

269 **Salt sensitivity of *957* is not due to interaction with LcpB but likely due to changes in**
270 **peptidoglycan crosslinking**

271 Since the gene *957* is on the same transcript as *lcpB* coding for a WTA ligase (Fig. 4B), the
272 contribution of WTA to salt stress resistance as well as the contribution of *957* to the attachment
273 of WTA to the cell wall was assessed. Initially the growth of a *tagO* (*tarO/llm*) mutant, a strain
274 unable to produce WTA, was tested in LB and LB 0.5 M NaCl medium. When cells were grown in
275 LB, they grew normally (Supplementary Fig. S8A), but under high salt conditions, the *tagO* mutant
276 showed reduced growth, similar to that of the *957* mutant (Fig. 5A). This is consistent with what
277 has been reported previously for a *Staphylococcus epidermidis tagO* mutant (Holland *et al.*, 2011)
278 and indicates an important role for WTA during salt stress. When the *lcpB* mutant was propagated
279 in LB medium, its growth was slightly inhibited (Supplementary Fig. S8A). However, in high salt
280 medium (Fig. 5A) it grew unimpeded and like WT. Since the *lcpB* mutant did not show a growth
281 defect in high salt medium, this made it unlikely that *957* is a regulator of LcpB activity, and hence
282 is involved in the attachment of WTA to the peptidoglycan. To specifically investigate the
283 requirement of 957 in WTA attachment, we isolated WTA from strains grown in either LB or LB
284 containing 0.4 M NaCl and separated the polymer on native polyacrylamide gels. The slightly lower
285 concentration of salt was chosen because growth of the *957* and the *tagO* mutants was too
286 strongly inhibited at 0.5 M NaCl. As expected the *tagO* mutant did not produce any WTA
287 (Supplementary Fig. S8B, Fig. 5B) and consistent with previous studies (Over *et al.*, 2011, Chan *et*
288 *al.*, 2013), the *lcpB* mutant exhibited slightly reduced WTA levels compared to the other strains
289 (Supplementary Fig. S8B, Fig. 5B). No reduction in WTA was observable in the *957* mutant

290 compared to the WT strain in either LB (Supplementary Fig. S8B & S8C) or LB 0.4 M NaCl (Fig. 5B &
291 5C) but rather a small increase, which could be complemented. Taken together, these data
292 indicate that 957 neither directly nor indirectly (e.g. through regulating the activity of LcpB) plays a
293 major role in WTA attachment.

294 Gene *957* is found upstream of the bi-functional autolysin gene *atl* and therefore we next
295 investigated potential changes in autolytic activity using zymograms. A small increase in autolytic
296 activity was detected in the *957* mutant (Fig. 5D) for bands around 55 kDa and 70 kDa compared
297 to the WT and complementation strain, indicating a possible change in Atl availability. We also
298 tested the susceptibility of the *957* mutant towards the cell wall active beta-lactam antibiotic
299 oxacillin. The *957* mutant exhibited a small but significant increase in MIC towards this antibiotic
300 compared to the WT and the complementation strain (Fig. 5E), indicating potential changes to the
301 peptidoglycan structure. To test this, we next analyzed the muropeptide profile of mutanolysin-
302 digested peptidoglycan isolated from the WT, the *957* mutant and complementation strain after
303 growth in LB or LB 0.4 M NaCl medium. Upon first inspection, no peaks were absent in any
304 condition or strain (Supplementary Fig. S8D and S8E). Probing further, mono- and multimers of
305 muropeptides up to 7-mers were quantified but no significant changes were found when strains
306 were cultured in LB medium (Fig. 6A). At the 0.4 M NaCl condition however, the muropeptide
307 profiles of the *957* mutant strain exhibited a significant decrease in the total amount of di- and
308 trimers and a significant increase in higher multimers compared to the WT and complementation
309 strain (Fig. 6B). This underlines the involvement of gene *957* in the cell wall homeostasis and
310 suggests that the sensitivity to NaCl could potentially be caused by higher crosslinking and possibly
311 rigidity of the peptidoglycan in the mutant.

312 **Salt-resistant suppressors possess variations in the transglycosylase domain of Pbp2**

313 Next, we attempted to generate *957* suppressor strains that showed improved growth in the
314 presence of 0.5 M NaCl, with the idea that by mapping and investigating the compensatory
315 mutations, further insight into the cellular functions of protein 957 could be gained. We readily
316 obtained suppressor strains by growth of the *957* mutant strain in NaCl containing liquid medium.
317 These strains grew as well as or even better than the WT LAC* strain in high salt conditions (Fig.
318 7A) and also grew similar to the WT in LB (Supplementary Fig. S9A). The genome sequences of 10
319 independent suppressor strains were determined and single nucleotide polymorphisms (SNPs) in
320 one or two genes could be identified for each strain (Supplementary Table S14), except for one
321 strain where the coverage was insufficient, and this strain was omitted from further analysis. A
322 common denominator for all suppressor strains were SNPs in the *pbp2* gene, coding for the
323 Penicillin binding protein 2 (Pbp2) (Fig. 7B). *S. aureus* Pbp2 is a bifunctional enzyme (Wyke, 1984,
324 Murakami *et al.*, 1994), which possesses transglycosylase and transpeptidase activity and is
325 involved in peptidoglycan synthesis. All nine discovered SNPs were unique and led to mutations in
326 the amino acid sequence in the transglycosylase domain but neither to stop codons, nor
327 frameshifts nor mutations in the transpeptidase domain. The mutations were mapped (Fig. 7B)
328 onto an available Pbp2 structure (3DWK) (Lovering *et al.*, 2008) to see if a specific area of the
329 transglycosylase domain had been targeted, but the amino acid substitutions were found
330 throughout the molecule and not only in the active site. Interestingly, also from the Tn-Seq data,
331 *pbp2* appeared to be considerably less important for growth at 0.5 M NaCl (Supplementary Fig.
332 S9B and S9C), although transposon insertions were mainly located at the beginning and end of the
333 gene or within the promoter region.

334 To confirm that the *pbp2* SNPs were indeed responsible for the suppression of the salt
335 sensitivity of the *957* mutant, we transferred the *pbp2* SNPs from two strains into a fresh
336 LAC*Δ*957* background by co-transduction of a transposon in a nearby gene (Supplementary Fig.

337 S9D, schematic). As expected, these "recreated" suppressor strains showed also increased salt
338 resistance (Fig. 7C, Supplementary Fig. S10A). In addition, we repaired the *pbp2* gene in two
339 suppressors to the WT *pbp2* allele and this reduced their ability to cope with NaCl stress, all
340 consistent with the hypothesis that the SNPs in *pbp2* are responsible for the suppression
341 phenotype (Fig. 7D, Supplementary Fig. S10B). When the same *pbp2* SNPs were transferred into a
342 WT LAC* strain, a reproducible growth improvement of the SNP-bearing strains was observed in
343 high salt medium, an indication that the *pbp2* mutations lead to a general growth improvement of
344 *S. aureus* under NaCl stress conditions (Fig. 7E, Supplementary Fig. S10C). Overall these results
345 show that several independent mutations in the *pbp2* gene can suppress the salt sensitivity of the
346 *957* mutant and can improve growth of the WT strain.

347 **Mutations in the *pbp2* gene alter moenomycin susceptibility and result in reduced peptidoglycan**
348 **crosslinking**

349 Moenomycin is a phosphoglycolipid antibiotic that inhibits the transglycosylase activity of the
350 *S. aureus* Pbp2 enzyme (reviewed in (Ostash & Walker, 2010)). To test if a decrease in Pbp2
351 transglycosylase activity results in improved growth of the *957* mutant in high salt conditions, cells
352 were grown on LB agar containing 0.5 M NaCl with or without moenomycin. The growth behaviors
353 of the WT strain and the *957* mutant were similar when grown on solid LB agar containing 0.5 M
354 NaCl but lacking moenomycin (Fig. 8A, top panel). This discrepancy in the growth behavior of the
355 *957* mutant in high salt liquid versus solid medium was already noted when we attempted to
356 generate suppressors on agar plates. On the other hand, in medium supplemented with 0.02
357 µg/ml moenomycin, we observed better growth of the *957* mutant compared to the WT strain
358 (Fig. 8A, lower panel). In addition, the *957* mutant also showed improved growth compared to the
359 two suppressor strains S2 and S4 when moenomycin was added (Fig. 8A, lower panel). These

360 findings are consistent with the idea that a partial inhibition of the glycosyltransferase activity of
361 Pbp2 can improve the growth of the *957* mutant in high salt medium.

362 Because the LAC*Δ*957* strain showed increased peptidoglycan crosslinking when compared to
363 a WT strain, we hypothesized that the peptidoglycan of the suppressor strains would be again less
364 crosslinked. To test this, the peptidoglycan from two of the suppressor strains grown in LB 0.4 M
365 NaCl was isolated, the muropeptide profiles determined and compared to that of the original *957*
366 mutant (Fig. 8B, Supplementary Fig. S10D). As before, the muropeptide profiles looked similar but
367 quantification revealed a significant reduction in crosslinked peptidoglycan fragments and a
368 significantly overrepresentation of monomeric and dimeric fragments in the suppressor strains as
369 compared to the original *957* mutant (Fig. 8B). These results indicate that the amount of
370 crosslinking of the peptidoglycan polymer is an important factor in the salt resistance of *S. aureus*
371 and that dysregulation of peptidoglycan crosslinking can lead to destabilizing effects.

372 **Discussion**

373 In this work, we performed TN-seq screens with *S. aureus* exposed to different osmotic
374 stresses and could show that each osmotic stressor affects a defined but different set of genes. It
375 is therefore important to use the term osmotic stress carefully, as our results highlight that there
376 is not one general osmotic stress response but rather responses tailored to the individual
377 osmolyte. Using the TN-seq method, we successfully identified several unknown salt tolerance
378 genes in *S. aureus* and further characterized gene *957,* a gene without previously assigned
379 function. Our results indicate that this gene product is involved in cell envelope homeostasis but
380 likely not WTA attachment and we show that its absence leads to increased crosslinking of the
381 peptidoglycan in the presence of NaCl. Suppressors of a *957* mutant acquired mutations in *pbp2*
382 and the increase in peptidoglycan crosslinking was reversed in such stains. This demonstrates that

383 the synthesis of the peptidoglycan layer is a tightly regulated process that plays an essential role
384 during osmotic stress.
385 TN-seq experiments track the growth ability of single mutants in a mixed population and can
386 therefore quickly and accurately determine genes that are required under certain growth
387 condition. It is however always a concern that a single TN-seq experiment might not be
388 reproducible due to stochastic extinction of individual mutants or certain growth dynamics. In this
389 study, we therefore performed two independent NaCl TN-seq experiments using two different
390 libraries and slightly different experimental setups. Although we detected differences between
391 experiments, overall the data proved to be rather consistent suggesting that a single experiment
392 would be sufficient in many cases.
393 From our TN-seq data and the use of different osmotic stressors (NaCl, KCl and sucrose), it is
394 evident that although all these compounds exert similar osmotic stresses, the responses differs
395 greatly between them (Figure 1 and Supplementary Figure S1-S2). NaCl and KCl conditions share a
396 set of genes that become essential such as *aapA* and *mgtE* but differ in the set of dispensable
397 genes. It is intriguing that a whole set of respiration related genes become dispensable under NaCl
398 stress but not under KCl stress. This could indicate that respiration should be inhibited or slowed
399 down in high NaCl conditions, possibly by interference with sodium pumps a process less likely to
400 be inhibited by potassium ions. The set of essential genes under sucrose conditions was vastly
401 different from that of the NaCl and KCl conditions whereas the set of sucrose dispensable genes
402 looked similar to the KCl set. This highlights the differences in osmotic stress adaptations and
403 serves as a reminder that the type of stressor remains important.
404 Most of the strains with mutations in genes we identified as NaCl essential in the TN-seq
405 screens, proved to be sensitive to 0.5 M NaCl, confirming the effectiveness of the TN-seq screens
406 (Supplementary Fig. S6). In particular, previously uncharacterized genes such as *SAUSA300_0694*,
407 *mgtE,* and the *957* gene could be identified as essential during NaCl stress and their phenotypes

408 could be complemented (Fig. 3). In our study, we opted not to experimentally validate any of the
409 dispensable genes, as the verification of a growth advantage is more difficult to prove than a
410 growth defect, but these genes will provide interesting starting points for future research. In
411 addition, it will be interesting to investigate higher concentrations of NaCl to see if the same or
412 different genes are flagged as essential and dispensable. Somewhat contradictory, our data
413 indicated, that the c-di-AMP phosphodiesterase enzymes GdpP and Pde2 are dispensable when
414 cells are exposed to high salt conditions. This is in contrast to the reports that construction and
415 propagation of a *dacA* mutant (coding for the cognate c-di-AMP cyclase DacA) is only possible at
416 high salt concentrations (or in defined chemical medium) (Zeden *et al.*, 2018). These findings do
417 however point to an involvement of c-di-AMP in salt mediated osmotic stress adaption in *S.*
418 *aureus*.

419 Gene *957* was selected for further characterization as part of this study, because it had
420 previously not been linked to NaCl stress and had not been investigated before. Initial tests
421 supported our proposed link to the cell envelope. The differences in CFU/OD correlations of the
422 WT and *957* mutant could be explained by the reduced cell size of the *957* mutant, as this would
423 produce more cells per OD unit. The underlying mechanism as to why *957* mutant cells are smaller
424 in size is still unclear but could be related to changes in peptidoglycan homeostasis.

425 As gene *957* is co-transcribed with *lcpB,* we initially assumed the encoded protein is involved
426 in WTA attachment via LcpB. However, we were unable to demonstrate such a link. Instead the
427 *957* mutant exhibited increased muropeptide crosslinking in the presence of 0.4 M NaCl, which
428 could be suppressed by *pbp2* SNPs suggesting an involvement in peptidoglycan synthesis. We can
429 only speculate if the SNPs identified in *pbp2* increase or inhibit the activity of Pbp2. However,
430 judging by the number of independent SNPs, it seems more likely that the mutations lead to a
431 decrease rather than an increase in transglycosylase activity. In addition, the results from the
432 moenomycin sensitivity experiments using a sublethal antibiotic concentration highlights that

433 partial inactivation of the transglycosylase activity of Pbp2 improves the growth of the *957* strain
434 in high salt conditions. This is consistent with the idea that the obtained *pbp2* SNPs lead to a
435 decrease in transglycosylase activity. The absence of frameshift or non-sense mutations can be
436 explained by the importance of the C-terminal transpeptidase domain of *pbp2* (Pinho *et al.*, 2001)
437 and this is also reflected in the transposon insertion distribution in *pbp2*. Intriguingly, the
438 suppressor mutants show reduced growth compared to the *957* mutant on moenomycin plates,
439 presumably due to transglycosylation activity being reduced to levels that are detrimental to the
440 cell. At this point it is unclear how mutations in the transglycosylase domain alter the muropeptide
441 pattern, since the peptide bonds are made by the transpeptidase, not the transglycosylase
442 domain. We hypothesize that a decrease in the efficiency of the glycosylation activity and slowing
443 down the glycan chain synthesis process will reduce the efficiency of the subsequent
444 transpeptidation process, resulting in decreased peptidoglycan crosslinking in the *pbp2* SNP
445 strains. It is also noteworthy that the *pbp2* gene becomes dispensable under NaCl conditions, an
446 additional indicator that Pbp2 activity needs to be avoided under high salt conditions.

447 Interestingly, the *957* mutant exhibited a slightly higher oxacillin MIC than the WT. This is in
448 contrast to what we expected as MICs are determined in 2% (0.342 M) salt medium and this
449 should lead to a growth disadvantage of the mutant. However, when seen in light of the increase
450 in peptidoglycan crosslinking, this could explain the growth advantage of the *957* mutant in the
451 presence of a beta-lactam antibiotic, as this could counter the inhibition of transpeptidases by
452 oxacillin.

453 Although we were unable to determine the exact molecular mechanism, it is clear from our
454 data that gene *957* is involved in cell wall synthesis either directly or indirectly. Based on these
455 data, we hypothesize that the rigidity of the peptidoglycan cell wall could be an important factor
456 to counter osmotic stresses, but further experimental work is needed to explore this in depth.

457 In conclusion, we have demonstrated differences between the osmotic stress response to
458 NaCl, KCl and sucrose in *S. aureus*. In addition, we identified a number of previously
459 uncharacterized factors involved in the osmotic stress response of *S. aureus,* which in particular
460 highlighted the importance of the cell envelope. The generated data will also provide a great
461 resource for further studies on the staphylococcal NaCl stress response.

462 **Experimental procedures**

463 **Growth of bacteria**

464 *E. coli* and *S. aureus* strains (see Supplementary Table S15 for details) were streaked from
465 frozen stocks onto Lysogenic Broth (LB) or Tryptic Soya agar (TSA) plates, respectively. For all *E.*
466 *coli* and most *S. aureus* experiments, the bacteria were grown in LB medium (Lennox Recipe: 10 g
467 Tryptone, 5 g Yeast extract, 5 g NaCl) pH 7.5 or LB medium with extra 0.5 M NaCl, 0.5 M KCl or 1.0
468 M Sucrose added. For molecular cloning and some other experiments (as indicated in the text), *S.*
469 *aureus* strains were grown in TSB medium. Growth curves were performed in 125 ml flasks with 20
470 ml of medium without antibiotics. Cultures were inoculated from overnight cultures to a starting
471 OD_{600} of 0.01 and growth was followed by determining OD_{600} readings every one or two hours.

472 **TN-seq experiments**

473 A previously published highly-saturated *S. aureus* USA300 library with a mix of six different
474 transposons was used (Santiago *et al.*, 2015, Coe *et al.*, 2019). In addition, a new transposon
475 library with only the blunt transposon, was produced using the same techniques as described
476 (Santiago *et al.*, 2015) containing approximately 1.2 million individual clones.
477 In the first experiment (NaCl, KCl and sucrose stress), a tube of the blunt library was thawed on ice
478 and used to set up a 20 ml pre-culture in LB/Erm 10 µg/ml with a starting OD_{600} of 0.1. This starter

479 culture was grown for 1 hour and subsequently used to inoculate 25 ml of either LB (Lennox
480 Recipe: 10 g Tryptone, 5 g Yeast extract, 5 g NaCl) pH 7.5 or LB with extra 0.5 M NaCl, extra 0.5 M
481 KCl or extra 1 M sucrose without Erm to a starting OD_{600} of 0.00125. When the cultures reached an
482 OD_{600} of approximately 0.3, the cultures were back-diluted 1:100-fold into 40 ml fresh medium
483 and 10-12 ml harvested by centrifugation when the back-diluted culture reached an OD_{600} of
484 approx. 1.0 (16 generations). The bacterial pellets were washed once with their respective growth
485 medium and stored at -20°C for further processing.
486 In the second experiment (NaCl, Replicate A), the multiplexed promoter transposon library was
487 used and Erm 5 µg/ml was added to the pre-culture and subsequent cultures in either LB (Lennox
488 Recipe: 10 g Tryptone, 5 g Yeast extract, 5 g NaCl) pH 7.5 or LB medium containing a final
489 concentration of 0.5 M NaCl. Samples were collected at an OD_{600} of about 1.4 (17 generations).
490 The third experiment (NaCl, replicate B) was set up similar to replicate A, however the blunt library
491 was used in this case and Erm 5 µg/ml was only added to the pre-culture.
492 The library preparation for sequencing was done as described previously (Santiago *et al.*,
493 2015). Briefly, genomic DNA was isolated, cut with *Not*I, biotinylated adapters ligated, the DNA cut
494 again with *Mme*I, and fragments ligated to Illumina adapters and the products PCR amplified,
495 incorporating bar codes and the Illumina adaptor sequences P5 and P7. The samples were
496 sequenced on an Illumina HiSeq machine after spiking with 40% PhiX DNA. The data analysis was
497 done using the Tufts Galaxy Server and custom python scripts as described earlier (Santiago *et al.*,
498 2015). To this end, the reads were trimmed up to the barcode and de-multiplexed by strain
499 barcode. Due to the variability in the DNA cleavage by the *Mme*I restriction enzyme, the reads that
500 could not be mapped to a barcode were trimmed by an additional base and the process repeated.
501 Reads were then mapped to the USA300_TCH1516 (CP000730.1) genome and a hop table was
502 generated. Statistical analysis (Mann-Whitney tests and Benjamini-Hochberg) was done using

503 custom python scripts (Santiago *et al.*, 2015). Further exploration of the data was done using Excel
504 and custom R scripts.

505 **_S. aureus_ cell diameter measurements**

506 For cell diameter measurements, *S. aureus* strains ANG4054, ANG4340, ANG4341 were grown
507 overnight (14-20 hours) at 37°C with 180 rpm shaking in 5 ml LB in the presence of 100 ng/ml Atet.
508 100 µl of these overnight cultures was transferred to a 1.5 ml reaction tube and 1.5 µl of BODIPY-
509 FL-vancomycin (100 µg/ml in phosphate buffered saline) was added to each tube to stain the cell
510 wall. After a 30 min static incubation step at 37°C, 1.5 µl of the suspension was pipetted onto a
511 slide covered with a 1% agarose pad and analyzed by microscopy using an Axio Imager.A2
512 microscope with an EC Plan-Neofluar 100x/1.30 Oil M27 objective and images recorded using an
513 AxioCam MR R3. Native CZI files were opened in FIJI (Schindelin *et al.*, 2012) and cell diameters of
514 200 cells were measured using the line and measure tool. Only cells without any visible septa were
515 measured. Experiment was conducted five times with independent biological cultures (n=5, 200
516 cells each).

517 **CFU/OD correlations**

518 The different *S. aureus* strains were grown as described for the cell diameter measurements.
519 Optical densities of cultures were measured as well as 100 µl of 10^{-6} dilutions (made in their
520 respective growth medium) plated onto TSA plates. The next day, the number of colonies were
521 counted and the ratios of OD_{600} to CFU calculated. The experiment was conducted six time with
522 independent biological samples (n=6).

523 **Zymogram assays**

524 The different *S. aureus* strains were grown over night in TSB. The next day, the bacteria from
525 an OD_{600} equivalent of 20 were pelleted by centrifugation for 3 min at 17000 x *g*. The cells were
526 washed twice with 600 µl PBS and subsequently suspended in 50 µl SDS sample buffer. The
527 suspension was boiled for 20 min with interspersed shaking, centrifuged for 5 min at 17000 x *g*
528 and 20 µl of each sample was loaded onto Zymogram gels, which where were prepared as
529 described previously (Atilano *et al.*, 2014). Gels were stained and de-stained using methylene blue
530 and water. The experiment was performed twice, and a representative result is shown.

531 **WTA isolation and analysis**

532 Overnight cultures of *S. aureus* strains ANG4054, ANG4340, ANG4341, ANG1575, ANG4290,
533 ANG4748, ANG4749, ANG4759 were prepared in LB and used to inoculate 50 ml LB or LB 0.4 M
534 NaCl to an OD_{600} of 0.01. The cultures were incubated at 37°C with shaking until they reached an
535 OD_{600} of 5 to 6. Where appropriate, 10 µg/ml chloramphenicol and 100 ng/ml Atet was also added
536 to the medium. The bacteria from 20-24 ml culture were harvested by centrifugation for 10 min at
537 7000 x *g*. The bacterial pellets were washed with 50 mM 2-(N-morpholino) ethanesulfonic acid
538 (MES) pH 6.5 buffer and stored at -20°C until further use. Pellets were then processed and WTA
539 separated on a 20% native polyacrylamide gel by electrophoresis on a Biorad Protein XL ii cell as
540 described previously (Covas *et al.*, 2016) and WTA visualized by silver staining according to the
541 manufacturer protocol. Experiments were done with three biological replicates (n=3) and a
542 representative result is shown.

543 **Peptidoglycan isolation and analysis**

544 Peptidoglycan was prepared as described previously (Corrigan *et al.*, 2011) with the following
545 modifications: 0.5 L (ANG4290, ANG4382, ANG4384) or 1.0 L (ANG5054, ANG4340, ANG4341) of
546 LB 0.4 M NaCl medium (all strains) or LB (ANG5054, ANG4340, ANG4341) medium were inoculated
547 to an OD_{600} of 0.01. For strains carrying derivatives of plasmid piTET, the medium was
548 supplemented with 100 ng/ml Atet starting from the pre-cultures. The cultures were grown at
549 37°C with shaking at 180 rpm until they reached an OD_{600} of 2-3 and bacteria were subsequently
550 harvested by centrifugation. Chromatography of mutanolysin digested peptidoglycan was
551 performed as described previously using an Agilent 1260 infinity system (Corrigan *et al.*, 2011) and
552 muropeptide peaks assigned according to de Jonge *et al.* (de Jonge *et al.*, 1992). For the
553 muropeptide quantification, a baseline was drawn, the total peak area determined as well as the
554 peak areas for mono- and the different multimer peaks and calculated as percentage of the total
555 peak area. The peak area quantification was done three times for each HPLC chromatogram and
556 average values were calculated. Experiments were done with three biological replicates (n=3).

557 **Data analysis, software and statistics**

558 Data were processed with a combination of Python 3.6 (https://www.python.org), R 3.3 & 3.5
559 (https://www.r-project.org/), RStudio 1.1 & 1.2 (https://www.rstudio.com/), Prism 7 and 8
560 (https://www.graphpad.com), ChemStation OpenLab C.01.05 (https://www.agilent.com/) and
561 Microsoft Excel 15 and 16 (https://www.office.com/). Microscopy images were analyzed using FIJI
562 1.0 (https://fiji.sc/). Statistical analysis was performed with Prism using appropriate tests as
563 described in the figure legends.

564 **Raising of Δ*957* suppressor strains**

565 Multiple independent overnight cultures of strain LAC*Δ*957* (ANG4290) were prepared in 5 ml
566 LB. These cultures were back diluted the next day into 20 ml LB 0.5 M NaCl to a starting OD_{600} of
567 0.05 and grown for 8-10 hours at 37°C with shaking until the cultures were slightly turbid. 50 µl of
568 each culture was passed into 5 ml of LB and grown overnight. The next day, appropriate culture
569 dilutions were plated onto LB agar plates and incubated overnight at 37°C. For each independent
570 culture, multiple single colonies were picked and used to inoculate individual wells of a 96-well
571 microtiter plates containing 100 µl LB and the plates were subsequently incubated at 37°C in a 96-
572 well plate incubator with shaking at 650 rpm. The next day, a culture aliquot was stored at -80°C,
573 and the cultures were also diluted 1:50 in LB 0.5 M NaCl medium and 20 µl of these diluted
574 cultures used to inoculate 180 µl of LB 0.5 M NaCl medium. The plates were incubated overnight
575 with shaking at 37°C and the next morning the growth of the potential *957* suppressor strains
576 compared to that of the original LAC*Δ*957* deletion strain (ANG4290), which showed low growth
577 and the WT LAC* (ANG1575) strain, which showed good growth. For each lineage, four
578 suppressors that showed good growth were streaked out from the previously frozen stocks and
579 subsequently single colonies selected to set up overnight cultures. The deletion of gene
580 *SAUSA300_0957* was confirmed by PCR and after performing growth curves in culture flasks, one
581 strain that showed significant growth improvement compared to the original LAC*Δ*957*
582 (ANG4290) strain was selected from each lineage. These strains were streaked out again for single
583 colonies and used to inoculate an overnight culture, giving rise to the independently raised
584 suppressor strains ANG4381 through ANG4394. The compensatory mutations for several of these
585 suppressor strains were subsequently determined by whole genome sequencing.

586 **Transfer of *pbp2* SNPs by phage transduction**

587 In order to demonstrate that the SNPs in *pbp2* are responsible for the growth rescue of strain
588 LAC*Δ*957* (ANG4290), we transferred two different *pbp2* SNPs by phage transduction into the
589 original LAC*Δ*957* strain as well as repaired these SNPs in the suppressor strains. This was done by
590 placing an Erm-marked transposon in proximity of the *pbp*2 gene allowing at a certain frequency
591 for the co-transduction of the Erm marker and the *pbp2* SNP. To this end, the NTML transposon
592 mutant library strain NE789 (Fey *et al.*, 2013) was used, which harbors a transposon insertion in
593 *SAUSA300_1332* (putative exonuclease) about 10 kbp upstream of the *pbp2* gene.
594 *SAUSA300_1332* is expected to be unrelated to salt stress and the cell wall synthesis machinery
595 but close enough to lead to an intermediate rate of co-transference with the *pbp2* SNPs. The
596 transposon from NE789 was transduced into WT LAC* (Boles *et al.*, 2010) and strain LAC*Δ*957*
597 (ANG4290) using phage Φ85 yielding strains ANG4561 and ANG452, respectively. The transposon
598 was also transduced into the suppressor strains ANG4382 and ANG4384 transferring either
599 *SAUSA300_1332::Tn* only, yielding strains ANG4527 and 4528 or transferring *SAUSA300_1332::Tn*
600 as well as replacing the *pbp2* SNP with a WT *pbp2* allele yielding *pbp2* repaired strains ANG4557
601 and ANG4568. Lysates from strains ANG4527 and 4528 (suppressors containing *pbp2* SNPs and
602 *SAUSA300_1332::Tn*) were used to transfer the *pbp2* SNPs back into a clean LAC*Δ*957* strain
603 background yielding strains ANG4624 and ANG4625 and into WT LAC*, yielding strains ANG4563
604 and ANG4564. Successful repair or transfer of the SNPs was checked by PCR and subsequent
605 restriction digest of the product choosing enzymes that recognize sites present in either the WT or
606 SNP allele (ANG4382 *pbp2* SNP: BsrI. Recognition site CCWGG, additional site introduced by SNP;
607 ANG4384 *pbp2* SNP: SspI. Recognition site: AATATT, site missing in SNP).

608 **Determination of oxacillin MICs using Etest strips**

609 *S. aureus* strains LAC* piTET (ANG4054), LAC*Δ*957* piTET (ANG4340) and the
610 complementation strain LAC*Δ*957* piTET-*957* (ANG4341) were grown overnight (22 hours) in 5 ml
611 TSB containing 10 µg/ml chloramphenicol and 100 ng/ml Atet. The next day, the cultures were
612 diluted to an OD_{600} of 0.1 in sterile PBS buffer and streaked with cotton swabs onto cation
613 adjusted Mueller-Hinton agar plates supplemented with 2% NaCl and 100 ng/ml Atet. One
614 M.I.C.Evaluator strip was placed on each plate and the plates were incubated for 24 hours at 35°C.
615 MICs were then read directly from the strips. The experiment was done with 4 biological replicates
616 (n=4).

617 **Moenomycin growth improvement test**

618 *S. aureus* strains LAC* (ANG1575), LAC* Δ*957* (ANG4290), LAC* Δ*957* S2 (ANG4382) and LAC*
619 Δ*957* S4 (ANG4384) were grown overnight (18 hours) in 5 ml LB. The next day, the cells were
620 diluted to an OD_{600} of 0.01 in LB, grown until mid-exponential phase (OD_{600} 0.4-0.6) and
621 normalized to an OD_{600} of 0.1. The cells were 10-fold serially diluted and 5 µl of each dilution
622 spotted onto LB agar containing 0.5 M NaCl with either 0.02 µg/ml moenomycin (mix of
623 moenomycin A, A12, C1, C3 and C4, Santa Cruz Biotechnology) or no moenomycin. Plates were
624 incubated at 37°C overnight (18-22 hours) and photographed. The experiment was done with 3
625 biological replicates (n=3) and one representative result is shown.

626 **Whole genome sequencing**

627 Genomic DNA was either isolated using the Promega Gene Wizard kit according to the
628 manufacturer instructions or using chloroform-isoamylalcohol as described previously (Schuster &
629 Bertram, 2014). DNA was sent off for whole genome sequencing to MicrobesNG, Birmingham, U.K.

630 or libraries prepared using the Illumina Nextera DNA kit and sequenced at the London Institute of
631 Medical Sciences. Short reads were trimmed in CLC workbench genomics (Qiagen), then mapped
632 to a custom *S. aureus* USA300 LAC* reference genome generated in a previous study (Bowman *et*
633 *al.*, 2016) and single nucleotide polymorphisms called based on at least 80% frequency of
634 occurrence. This list was compared to a manually curated list of well non false-positives and these
635 entries were removed.

636 **Nebraska Transposon Mutant Library (NTML) strains and complementation strains**

637 All Nebraska transposon mutant library (NTML) strains and primers used in this study are
638 listed in Supplementary Tables S13, S15 and S16. Transposon insertions in the respective genes
639 were confirmed by PCRs. For complementation analysis, NTML strains NE535 (JE2
640 *SAUSA300_0867*::*Tn*), NE867 (JE2 *SAUSA300_0483*::*Tn*) were transformed as controls with the
641 empty plasmid pCL55 (Lee *et al.*, 1991), yielding strains ANG4326 and ANG4328 and strains NE188
642 (JE2 *SAUSA300_0481*::*Tn*), NE251 (JE2 SAUSA300_0482::*Tn*), NE526 (JE2 *SAUSA300_0694*::*Tn*),
643 NE736 (JE2 *SAUSA300_0910*::*Tn*), NE1384 (JE2 *SAUSA300_0957*::*Tn*) with plasmid piTET (Gründling
644 & Schneewind, 2007), yielding ANG4308, ANG4310, ANG4377, ANG4336, ANG4338. The WT strain
645 JE2 (Fey *et al.*, 2013) was also transformed with both plasmids yielding JE2 pCL55 (ANG4325) and
646 JE2 piTET (ANG4307).

647 The complementation plasmid piTET-*481* for strain NE188 (JE2 *SAUSA300_0481*::*Tn*) was
648 constructed by amplifying the *SAUSA300_0481* gene using primers P2378/P2379, digesting the
649 product with AvrII/BglII and ligating the fragment with plasmid piTET cut with the same enzymes.
650 The plasmid was then introduced into *E. coli* strain XL1-Blue, yielding ANG4139. After shuttling the
651 plasmid through *E. coli* strain IM08B (Monk *et al.*, 2012), creating strain ANG4150, the plasmid was
652 integrated into the *geh* locus of NE188 (JE2 *SAUSA300_0481*::*Tn*) yielding strain ANG4309. The
653 complementation plasmid piTET-*482* for strain NE251 (JE2 SAUSA300_0482::*Tn*), piTET-*694* for

654 strain NE526 (JE2 *SAUSA300_0694*::*Tn*), piTET-*910* for strain NE736 (JE2 *SAUSA300_0910*::*Tn*), and
655 piTET-*957* for strain NE1384 (JE2 *SAUSA300_0957*::*Tn*) were constructed in a similar manner using
656 primer pairs P2380/P2381 (*SAUSA300_0482*), P2388/P2389 (*SAUSA300_0694*), P2384/P2385
657 (*SAUSA300_0910*) and P2386/P2387 (*SAUSA300_0957*), respectively. The complementation
658 plasmids were recovered in *E. coli* XL1-Blue yielding strains ANG4140 (SAUSA300_0482), ANG4142
659 (*SAUSA300_0694*), ANG4144 (*SAUSA300_0910*) and ANG4145 (*SAUSA300_0957*), shuttled through
660 *E. coli* IM08B giving strains ANG4151 (*SAUSA300_0482*), ANG4153 (*SAUSA300_0694*), ANG4155
661 (*SAUSA300_0910*) and ANG4156 (*SAUSA300_0957*) and finally introduced in the respective NTML
662 strain yielding the complementation strains ANG4311 (*SAUSA300_0482*), ANG4378
663 (*SAUSA300_0694*), ANG4337 (*SAUSA300_0910*) and ANG4339 (*SAUSA300_0957*).

664 Complementation plasmid pCL55-*483* for strain NE867 (JE2 *SAUSA300_0483*::*Tn*) was made by
665 fusing PCR products of the operon promoter (in front of *SAUSA300_0481*) amplified with primers
666 P2588/P2553 and the *SAUSA300_0483* gene, amplified with primers P2554/P2589 together using
667 primers P2588/P2589. The resulting fragment was cloned into pCL55 using EcoRI/BamHI
668 restriction sites. The plasmid was recovered in XL1-Blue, creating strain ANG4291, shuttled
669 through *E. coli* IM08B (ANG4292) and subsequently introduced into NE867 (JE2
670 *SAUSA300_0483*::*Tn*) to create strain ANG4327. The complementation plasmid pCL55-*867* for
671 strain NE535 (JE2 *SAUSA300_0867*::*Tn*) was constructed in a similar manner, using primers
672 P2590/P2556 and P2557/P2591 to amplify the promoter and *SAUSA300_0867* gene, which were
673 subsequently fused in a second PCR using primers P2590/P2591. The resulting fragment was
674 cloning into pCL55 using EcoRI/BamHI restriction sites and the resulting plasmid recovered in *E.*
675 *coli* XL1-Blue (ANG4293), shuttling through IM08B (ANG4294) and finally introduced into NE535
676 (JE2 *SAUSA300_0867*::*Tn*), creating the complementation strain ANG4329.

677 **Construction of *S. aureus* gene deletion and complementation strains**

678 *S. aureus* strains with in-frame gene deletions were constructed by allelic exchange using
679 plasmids pIMAY (Monk *et al.*, 2012) and pIMAY* (Schuster *et al.*, 2019). The gene deletion
680 plasmids were designed to contain approximately 1000 bp up- and downstream regions around
681 the deletion site, amplified from LAC* genomic DNA (Boles *et al.*, 2010), and the first and last 30
682 bp of the open reading frame to be deleted.

683 For construction of plasmid pIMAY-Δ*957*, the up- and downstream regions of *SAUSA300_0957*
684 were amplified using primers P2370/P2371 and P2372/P2373, spliced together in a second PCR
685 using primers P2370/P2373 and cloned into pIMAY using XmaI/EcoRI. Plasmid pIMAY-Δ957 was
686 recovered in *E. coli* XL1-Blue, creating strain ANG4147, shuttled through *E. coli* IM08B (ANG4159)
687 and subsequently introduced into S. *aureus* LAC*Δ*957*. The allelic exchange to delete
688 *SAUSA300_0957* and to create strain LAC*Δ*957* (ANG4290) was performed as previously described
689 (Monk *et al.*, 2012). For complementation analysis, plasmid piTET-*957* was integrated into the
690 chromosome of strain LAC*Δ*957*, giving rise to the complementation strain LAC*Δ*957* piTET-*957*
691 (ANG4341). As control, the empty plasmid piTET from ANG4163 was also integrated into the
692 chromosome of LAC*Δ*957* yielding strain LAC*Δ*957* piTET (ANG4340). The *lcpB* (SAUSA300_0958)
693 gene was deleted in a similar manner using primers P2844/P2845 and P2846/P2847 for the first
694 and primers P2844/P2847 for the second PCR and cloning the fragment XmaI/EcoRI into pIMAY.
695 Plasmid pIMAY-Δ*lcpB* was recovered in *E. coli* XL1blue (ANG4740), shuttled through *E. coli* IM08B
696 (ANG4742) and introduced into the *S. aureus* LAC* (ANG4744) and finally yielding the *lcpB*
697 deletion strain LAC*Δ*lcpB* (ANG4748).

698 Plasmid pIMAY*-Δ*957-958* was constructed for the production of an *SAUSA300_0957-0958*
699 (*lcpB*) double mutant strain in which the first 30 bases of *SAUSA300_0957* were fused to the last
700 30 bp of *SAUSA300_0958* (*lcpB*). This was done using primers P2844/P2848 and P2849/P2373 in
701 the first and primers P2844/P2373 in a second PCR. The fragment was cloned using XmaI/EcoRI

702 into pIMAY* (Schuster *et al.*, 2019) and the resulting plasmid pIMAY*-Δ*957-958* recovered in *E.*
703 *coli* XL1-Blue (ANG4741). The plasmid was shuttled through *E. coli* IM08B (ANG4743), introduced
704 into *S. aureus* LAC* (ANG4745) and following the allelic exchange procedure yielding the *S. aureus*
705 strain LAC*Δ*957-958* (*lcpB*) (ANG4749).

706 The plasmid pIMAY-Δ*mgtE* was designed to contain up- and downstream regions of
707 *SAUSA300_0910* (*mgtE*) fused together by the first and last 30 bp of the gene in order to create a
708 LAC*Δ*mgtE* mutant. For this, primer pairs P2374/P2375 and P2376/P2377 were used to amplify
709 up- and downstream regions and subsequently spliced together by PCR using primers
710 P2374/P2377. The PCR fragment was digested with XmaI/EcoRI and ligated into pIMAY cut with
711 the same enzymes. The plasmid pIMAY-Δ*mgtE* was recovered in *E. coli* XL1-Blue yielding strain
712 ANG4146 and shuttled through *E. coli* IM08B yielding strain ANG4158. The plasmid pIMAY-Δ*mgtE*
713 was then introduced into LAC* yielding strain LAC*Δ*SAUSA300_0910* (*mgtE*) (ANG4422) after the
714 knockout procedure. To create an empty vector-containing control strain and a plasmid-based
715 complementation strain, the plasmid piTET and piTET-*910* from strains ANG4163 and ANG4155
716 were isolated and used to transform strain LAC*Δ*SAUSA300_0910* (*mgtE*) (ANG4422), yielding
717 strains ANG4445 (LAC*Δ*mgtE* piTET) and ANG4446 (LAC*Δ*mgtE* piTET-*mgtE)*.

718 The *tagO* gene (*SAUSA300_0731*) was inactivated using the targetron intron homing system
719 (Yao *et al.*, 2006) or by allelic exchange using pIMAY* (Schuster *et al.*, 2019). For the targetron
720 mutagenesis, plasmid pNL9164-*tagO* was produced by amplifying the upstream targetron
721 fragment with primers P2887 and the EBS universal primer (P2890) and the downstream fragment
722 using primers P2888/P2889, the fragments were fused using the IBS primer (P2887) and the EBS1d
723 primer (P2888). The final fragment was cloned using HindIII/BsrGI into pNL9164 (Yao *et al.*, 2006).
724 Plasmid pNL9164-*tagO* was recovered in *E. coli* XL1-Blue, yielding strain ANG4703, introduced into
725 *E. coli* IM08B to give rise to strain ANG4704 and finally introduced into *S. aureus* LAC* (Boles *et al.*,
726 2010) to create strain LAC* pNL9164-*tagO* (ANG4751). The final *tagO* targetron mutant strain

727 LAC**tagO*::targetron (ANG4753) was generated using the method described by Yao *et al.* (Yao *et*
728 *al.*, 2006). For the construction of *S. aureus* strain LAC*Δ*tagO* with an in-frame deletion in *tagO,*
729 the allelic exchange plasmid pIMAY*-Δ*tagO* was used. To this end, up- and downstream *tagO*
730 fragments were produced using primer pairs P2883/P2884 and P2885/P2886 and introduced by
731 Gibson cloning into XmaI/EcoRI pre-cut pIMAY*. Plasmid pIMAY*-Δ*tagO* was recovered in *E. coli*
732 XL1-Blue, generating strain ANG4755. After shuttling through *E. coli* strain IM08B (ANG4756), the
733 plasmid was introduced into *S. aureus* LAC* to create strain ANG4757. Finally, the *tagO* locus was
734 deleted by allelic exchange, generating strain LAC*Δ*tagO* (ANG4759). Because initial generation of
735 the mutant failed, cells were plated unselectively onto TSA plates and incubated at room
736 temperature (18-25°C) for about two weeks to enable colony differentiation between WT and
737 Δ*tagO* mutant strains. Upon prolonged incubation, *tagO* mutant strain colonies have an opaque
738 appearance.

739 **Data access**

740 The whole genome sequencing data were deposited at the European Nucleotide Archive
741 (ENA) under accession id ERP115099 and TN-seq data in the short read archive (SRA) at the
742 National Center for Biotechnology Information (NCBI) under BioProject ID PRJNA544248. Analyzed
743 tables can be found in the supplementary files. For other data, please contact the corresponding
744 author.

745 **Acknowledgements**

746 This research was funded by the Wellcome Trust through grants 100289 and 210671/Z/18/Z
747 to A.G. and the NIH grant P01AI083214 to S.W.. C.F.S. was supported by the German Research
748 Foundation [Deutsche Forschungsgemeinschaft (DFG)] through grant SCHU 3159/1–1 and F.C.M.K.
749 by a Wellcome trust Ph.D. studentship. The funders had no role in study design, data collection

750 and analysis, decision to publish, or preparation of the manuscript. We thank Microbes NG and the
751 London Institute of Medical Sciences for providing whole genome sequencing services and the
752 Tufts sequencing facility for the sequencing services for the TN-seq experiments. We also would
753 like to thank Ute Bertsche for kind advice on HPLC analyses.

754 **Author contributions**

755 C.F.S., D.M.W., F.C.K. and A.G. performed the research; C.F.S., D.M.W., F.C.M.K., M.S., S.W.
756 and A.G. analyzed the data; C.F.S. and A.G. designed the research; C.F.S. and A.G. wrote the paper.
757 All authors approved the final version of the manuscript.
758

759 **Disclosure declaration**

760 The authors declare not conflict of interest.

761 **Graphical abstract**

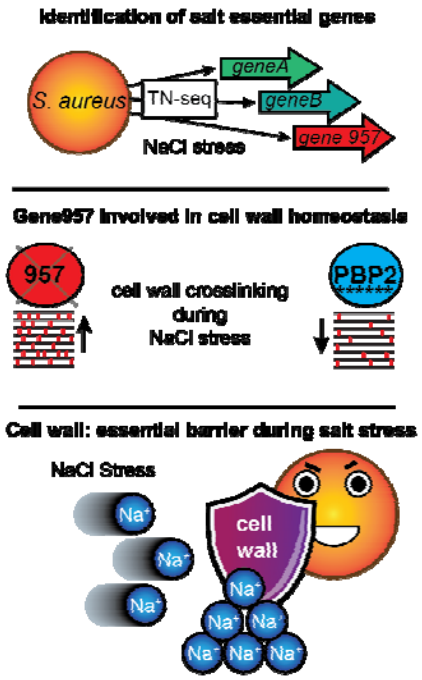

762

763 **Abbreviated summary**

764 *Staphylococcus aureus* is able to grow in the presence of high concentrations of NaCl but the
765 exact genetic factors contributing to this are unknown. Using a high-throughput TN-seq approach,
766 we identified gene *957* as an important factor for the salt stress resistance in *S. aureus*. A *957*-
767 mutant was not only salt sensitive but also showed increased peptidoglycan crosslinking,
768 altogether highlighting the cell wall as an important barrier against osmotic stress.

769

770

771 **References**

772 Adams, M.R., and Moss, M.O., (2008) 7.14.2 The Organism and its Characteristics. In: Food
773 Microbiology (3rd Edition). Royal Society of Chemistry, pp.
774 Anderson, C.B., and Witter, L.D. (1982) Glutamine and proline accumulation by *Staphylococcus*
775 *aureus* with reduction in water activity. *Appl Environ Microbiol* **43**: 1501-1503.
776 Atilano, M.L., Pereira, P.M., Vaz, F., Catalão, M.J., Reed, P., Grilo, I.R., Sobral, R.G., Ligoxygakis, P.,
777 Pinho, M.G., and Filipe, S.R. (2014) Bacterial autolysins trim cell surface peptidoglycan to
778 prevent detection by the *Drosophila* innate immune system. *Elife* **3**: e02277.
779 Bae, J.H., and Miller, K.J. (1992) Identification of two proline transport systems in *Staphylococcus*
780 *aureus* and their possible roles in osmoregulation. *Appl Environ Microbiol* **58**: 471-475.
781 Berger-Bächi, B., Barberis-Maino, L., Strässle, A., and Kayser, F.H. (1989) FemA, a host-mediated
782 factor essential for methicillin resistance in *Staphylococcus aureus*: molecular cloning and
783 characterization. *Mol Gen Genet* **219**: 263-269.
784 Boles, B.R., Thoendel, M., Roth, A.J., and Horswill, A.R. (2010) Identification of genes involved in
785 polysaccharide-independent *Staphylococcus aureus* biofilm formation. *PLoS One* **5**: e10146.
786 Booth, I.R. (2014) Bacterial mechanosensitive channels: progress towards an understanding of
787 their roles in cell physiology. *Curr Opin Microbiol* **18**: 16-22.
788 Bowman, L., Zeden, M.S., Schuster, C.F., Kaever, V., and Grundling, A. (2016) New Insights into the
789 Cyclic Di-adenosine Monophosphate (c-di-AMP) Degradation Pathway and the
790 Requirement of the Cyclic Dinucleotide for Acid Stress Resistance in *Staphylococcus aureus*.
791 *J Biol Chem* **291**: 26970-26986.
792 Bremer, E., and Krämer, R. (2019) Responses of Microorganisms to Osmotic Stress. *Annu Rev*
793 *Microbiol* **73**: 313-334.
794 Brown, S., Santa Maria, J.P., Jr., and Walker, S. (2013) Wall teichoic acids of gram-positive bacteria.
795 *Annu Rev Microbiol* **67**: 313-336.
796 Chan, Y.G., Frankel, M.B., Dengler, V., Schneewind, O., and Missiakas, D. (2013) *Staphylococcus*
797 *aureus* mutants lacking the LytR-CpsA-Psr family of enzymes release cell wall teichoic acids
798 into the extracellular medium. *J Bacteriol* **195**: 4650-4659.
799 Chan, Y.G., Kim, H.K., Schneewind, O., and Missiakas, D. (2014) The capsular polysaccharide of
800 *Staphylococcus aureus* is attached to peptidoglycan by the LytR-CpsA-Psr (LCP) family of
801 enzymes. *J Biol Chem* **289**: 15680-15690.
802 Christian, J.H., and Waltho, J.A. (1964) The Composition of *Staphylococcus aureus* in Relation to
803 the Water Activity of the Growth Medium. *J Gen Microbiol* **35**: 205-213.
804 Coe, K.A., Lee, W., Komazin-Meredith, G., Meredith, T.C., Grad, Y.H., and Walker, S. (2019)
805 Comparative Tn-Seq reveals common daptomycin resistance determinants in
806 *Staphylococcus aureus* despite strain-dependent differences in essentiality of shared cell
807 envelope genes. *bioRxiv*: 648246.
808 Commichau, F.M., Gibhardt, J., Halbedel, S., Gundlach, J., and Stülke, J. (2018) A Delicate
809 Connection: c-di-AMP Affects Cell Integrity by Controlling Osmolyte Transport. *Trends*
810 *Microbiol* **26**: 175-185.
811 Corrigan, R.M., Abbott, J.C., Burhenne, H., Kaever, V., and Gründling, A. (2011) c-di-AMP is a new
812 second messenger in *Staphylococcus aureus* with a role in controlling cell size and envelope
813 stress. *PLoS Pathog* **7**: e1002217.
814 Corrigan, R.M., Campeotto, I., Jeganathan, T., Roelofs, K.G., Lee, V.T., and Gründling, A. (2013)
815 Systematic identification of conserved bacterial c-di-AMP receptor proteins. *Proc Natl Acad*
816 *Sci U S A* **110**: 9084-9089.
817 Corrigan, R.M., and Gründling, A. (2013) Cyclic di-AMP: another second messenger enters the fray.
818 *Nat Rev Microbiol* **11**: 513-524.

819 Covas, G., Vaz, F., Henriques, G., Pinho, M.G., and Filipe, S.R. (2016) Analysis of Cell Wall Teichoic
820 Acids in *Staphylococcus aureus*. *Methods Mol Biol* **1440**: 201-213.
821 Cox, C.D., Bavi, N., and Martinac, B. (2018) Bacterial Mechanosensors. *Annu Rev Physiol* **80**: 71-93.
822 Csonka, L.N. (1989) Physiological and genetic responses of bacteria to osmotic stress. *Microbiol*
823 *Rev* **53**: 121-147.
824 Csonka, L.N., and Hanson, A.D. (1991) Prokaryotic osmoregulation: genetics and physiology. *Annu*
825 *Rev Microbiol* **45**: 569-606.
826 de Jonge, B.L., Chang, Y.S., Gage, D., and Tomasz, A. (1992) Peptidoglycan composition of a highly
827 methicillin-resistant *Staphylococcus aureus* strain. The role of penicillin binding protein 2A.
828 *J Biol Chem* **267**: 11248-11254.
829 Fey, P.D., Endres, J.L., Yajjala, V.K., Widhelm, T.J., Boissy, R.J., Bose, J.L., and Bayles, K.W. (2013) A
830 genetic resource for rapid and comprehensive phenotype screening of nonessential
831 *Staphylococcus aureus* genes. *MBio* **4**: e00537-00512.
832 Graham, J.E., and Wilkinson, B.J. (1992) *Staphylococcus aureus* osmoregulation: roles for choline,
833 glycine betaine, proline, and taurine. *J Bacteriol* **174**: 2711-2716.
834 Gründling, A., and Schneewind, O. (2007) Genes required for glycolipid synthesis and lipoteichoic
835 acid anchoring in *Staphylococcus aureus*. *J Bacteriol* **189**: 2521-2530.
836 Gunde-Cimerman, N., Plemenitas, A., and Oren, A. (2018) Strategies of adaptation of
837 microorganisms of the three domains of life to high salt concentrations. *FEMS Microbiol*
838 *Rev* **42**: 353-375.
839 Holland, L.M., Conlon, B., and O'Gara, J.P. (2011) Mutation of *tagO* reveals an essential role for
840 wall teichoic acids in *Staphylococcus epidermidis* biofilm development. *Microbiology* **157**:
841 408-418.
842 Jordan, S., Hutchings, M.I., and Mascher, T. (2008) Cell envelope stress response in Gram-positive
843 bacteria. *FEMS Microbiol Rev* **32**: 107-146.
844 Kho, K., and Meredith, T.C. (2018) Salt-Induced Stress Stimulates a Lipoteichoic Acid-Specific
845 Three-Component Glycosylation System in *Staphylococcus aureus*. *J Bacteriol* **200**.
846 Koprivnjak, T., Mlakar, V., Swanson, L., Fournier, B., Peschel, A., and Weiss, J.P. (2006) Cation-
847 induced transcriptional regulation of the dlt operon of *Staphylococcus aureus*. *J Bacteriol*
848 **188**: 3622-3630.
849 Lee, C.Y., Buranen, S.L., and Ye, Z.H. (1991) Construction of single-copy integration vectors for
850 *Staphylococcus aureus*. *Gene* **103**: 101-105.
851 Lovering, A.L., De Castro, L., and Strynadka, N.C. (2008) Identification of dynamic structural motifs
852 involved in peptidoglycan glycosyltransfer. *J Mol Biol* **383**: 167-177.
853 Mäder, U., Nicolas, P., Depke, M., Pané-Farré, J., Debarbouille, M., van der Kooi-Pol, M.M., Guérin,
854 C., Dérozier, S., Hiron, A., Jarmer, H., Leduc, A., Michalik, S., Reilman, E., Schaffer, M.,
855 Schmidt, F., Bessières, P., Noirot, P., Hecker, M., Msadek, T., Völker, U., and van Dijl, J.M.
856 (2016) *Staphylococcus aureus* Transcriptome Architecture: From Laboratory to Infection-
857 Mimicking Conditions. *PLoS Genet* **12**: e1005962.
858 Madiraju, M.V., Brunner, D.P., and Wilkinson, B.J. (1987) Effects of temperature, NaCl, and
859 methicillin on penicillin-binding proteins, growth, peptidoglycan synthesis, and autolysis in
860 methicillin-resistant *Staphylococcus aureus*. *Antimicrob Agents Chemother* **31**: 1727-1733.
861 Mayer, S., Steffen, W., Steuber, J., and Götz, F. (2015) The *Staphylococcus aureus* NuoL-like protein
862 MpsA contributes to the generation of membrane potential. *J Bacteriol* **197**: 794-806.
863 Measures, J.C. (1975) Role of amino acids in osmoregulation of non-halophilic bacteria. *Nature*
864 **257**: 398-400.
865 Miller, K.J., Zelt, S.C., and Bae, J.-H. (1991) Glycine betaine and proline are the principal compatible
866 solutes of *Staphylococcus aureus*. *Current Microbiology* **23**: 131-137.

867 Mistretta, N., Brossaud, M., Telles, F., Sanchez, V., Talaga, P., and Rokbi, B. (2019) Glycosylation of
868 *Staphylococcus aureus* cell wall teichoic acid is influenced by environmental conditions. *Sci*
869 *Rep* **9**: 3212.
870 Mitchell, P., and Moyle, J. (1959) Permeability of the envelopes of *Staphylococcus aureus* to some
871 salts, amino acids, and non-electrolytes. *J Gen Microbiol* **20**: 434-441.
872 Monk, I.R., Shah, I.M., Xu, M., Tan, M.W., and Foster, T.J. (2012) Transforming the
873 untransformable: application of direct transformation to manipulate genetically
874 *Staphylococcus aureus* and *Staphylococcus epidermidis*. *MBio* **3**.
875 Murakami, K., Fujimura, T., and Doi, M. (1994) Nucleotide sequence of the structural gene for the
876 penicillin-binding protein 2 of *Staphylococcus aureus* and the presence of a homologous
877 gene in other staphylococci. *FEMS Microbiol Lett* **117**: 131-136.
878 Ochiai, T. (2000) *Staphylococcus aureus* produces autolysin-susceptible cell walls during growth in
879 a high-NaCl and low-Ca2+ concentration medium. *Microbiol Immunol* **44**: 97-104.
880 Onyango, L.A., Hugh Dunstan, R., Roberts, T.K., Macdonald, M.M., and Gottfries, J. (2013)
881 Phenotypic variants of staphylococci and their underlying population distributions
882 following exposure to stress. *PLoS One* **8**: e77614.
883 Oshida, T., Sugai, M., Komatsuzawa, H., Hong, Y.M., Suginaka, H., and Tomasz, A. (1995) A
884 *Staphylococcus aureus* autolysin that has an N-acetylmuramoyl-L-alanine amidase domain
885 and an endo-beta-N-acetylglucosaminidase domain: cloning, sequence analysis, and
886 characterization. *Proc Natl Acad Sci U S A* **92**: 285-289.
887 Ostash, B., and Walker, S. (2010) Moenomycin family antibiotics: chemical synthesis, biosynthesis,
888 and biological activity. *Nat Prod Rep* **27**: 1594-1617.
889 Over, B., Heusser, R., McCallum, N., Schulthess, B., Kupferschmied, P., Gaiani, J.M., Sifri, C.D.,
890 Berger-Bächi, B., and Stutzmann Meier, P. (2011) LytR-CpsA-Psr proteins in *Staphylococcus*
891 *aureus* display partial functional redundancy and the deletion of all three severely impairs
892 septum placement and cell separation. *FEMS Microbiol Lett* **320**: 142-151.
893 Pinho, M.G., Filipe, S.R., de Lencastre, H., and Tomasz, A. (2001) Complementation of the essential
894 peptidoglycan transpeptidase function of penicillin-binding protein 2 (PBP2) by the drug
895 resistance protein PBP2A in *Staphylococcus aureus*. *J Bacteriol* **183**: 6525-6531.
896 Pöhlmann-Dietze, P., Ulrich, M., Kiser, K.B., Döring, G., Lee, J.C., Fournier, J.M., Botzenhart, K., and
897 Wolz, C. (2000) Adherence of *Staphylococcus aureus* to endothelial cells: influence of
898 capsular polysaccharide, global regulator agr, and bacterial growth phase. *Infect Immun* **68**:
899 4865-4871.
900 Pourkomailian, B., and Booth, I.R. (1992) Glycine betaine transport by *Staphylococcus aureus*:
901 evidence for feedback regulation of the activity of the two transport systems. *Microbiology*
902 **140 (Pt 11)**: 3131-3138.
903 Price-Whelan, A., Poon, C.K., Benson, M.A., Eidem, T.T., Roux, C.M., Boyd, J.M., Dunman, P.M.,
904 Torres, V.J., and Krulwich, T.A. (2013) Transcriptional profiling of *Staphylococcus aureus*
905 during growth in 2 M NaCl leads to clarification of physiological roles for Kdp and Ktr K+
906 uptake systems. *MBio* **4**.
907 Rahman, M.M., Hunter, H.N., Prova, S., Verma, V., Qamar, A., and Golemi-Kotra, D. (2016) The
908 *Staphylococcus aureus* Methicillin Resistance Factor FmtA Is a d-Amino Esterase That Acts
909 on Teichoic Acids. *MBio* **7**: e02070-02015.
910 Santiago, M., Matano, L.M., Moussa, S.H., Gilmore, M.S., Walker, S., and Meredith, T.C. (2015) A
911 new platform for ultra-high density *Staphylococcus aureus* transposon libraries. *BMC*
912 *Genomics* **16**: 252.
913 Schaefer, K., Matano, L.M., Qiao, Y., Kahne, D., and Walker, S. (2017) In vitro reconstitution
914 demonstrates the cell wall ligase activity of LCP proteins. *Nat Chem Biol* **13**: 396-401.

915 Schindelin, J., Arganda-Carreras, I., Frise, E., Kaynig, V., Longair, M., Pietzsch, T., Preibisch, S.,
916 Rueden, C., Saalfeld, S., Schmid, B., Tinevez, J.Y., White, D.J., Hartenstein, V., Eliceiri, K.,
917 Tomancak, P., and Cardona, A. (2012) Fiji: an open-source platform for biological-image
918 analysis. *Nat Methods* **9**: 676-682.
919 Schuster, C.F., Bellows, L.E., Tosi, T., Campeotto, I., Corrigan, R.M., Freemont, P., and Gründling, A.
920 (2016) The second messenger c-di-AMP inhibits the osmolyte uptake system OpuC in
921 *Staphylococcus aureus*. *Sci Signal* **9**: ra81.
922 Schuster, C.F., and Bertram, R. (2014) Fluorescence based primer extension technique to
923 determine transcriptional starting points and cleavage sites of RNases *in vivo*. *J Vis Exp*:
924 e52134.
925 Schuster, C.F., Howard, S.A., and Gründling, A. (2019) Use of the counter selectable marker PheS*
926 for genome engineering in *Staphylococcus aureus*. *Microbiology*.
927 Schwan, W.R., Lehmann, L., and McCormick, J. (2006) Transcriptional activation of the
928 *Staphylococcus aureus* putP gene by low-proline-high osmotic conditions and during
929 infection of murine and human tissues. *Infect Immun* **74**: 399-409.
930 Scybert, S., Pechous, R., Sitthisak, S., Nadakavukaren, M.J., Wilkinson, B.J., and Jayaswal, R.K.
931 (2003) NaCl-sensitive mutant of *Staphylococcus aureus* has a Tn917-lacZ insertion in its ars
932 operon. *FEMS Microbiol Lett* **222**: 171-176.
933 Sleator, R.D., and Hill, C. (2002) Bacterial osmoadaptation: the role of osmolytes in bacterial stress
934 and virulence. *FEMS Microbiol Rev* **26**: 49-71.
935 Stapleton, M.R., Horsburgh, M.J., Hayhurst, E.J., Wright, L., Jonsson, I.M., Tarkowski, A., Kokai-Kun,
936 J.F., Mond, J.J., and Foster, S.J. (2007) Characterization of IsaA and SceD, two putative lytic
937 transglycosylases of *Staphylococcus aureus*. *J Bacteriol* **189**: 7316-7325.
938 Stewart, C.M., Cole, M.B., Legan, J.D., Slade, L., and Schaffner, D.W. (2005) Solute-specific effects
939 of osmotic stress on *Staphylococcus aureus*. *J Appl Microbiol* **98**: 193-202.
940 Stewart, C.M., Cole, M.B., Legan, J.D., Slade, L., Vandeven, M.H., and Schaffner, D.W. (2002)
941 *Staphylococcus aureus* growth boundaries: moving towards mechanistic predictive models
942 based on solute-specific effects. *Appl Environ Microbiol* **68**: 1864-1871.
943 Tong, S.Y., Davis, J.S., Eichenberger, E., Holland, T.L., and Fowler, V.G., Jr. (2015) *Staphylococcus*
944 *aureus* infections: epidemiology, pathophysiology, clinical manifestations, and
945 management. *Clin Microbiol Rev* **28**: 603-661.
946 Townsend, D.E., and Wilkinson, B.J. (1992) Proline transport in *Staphylococcus aureus*: a high-
947 affinity system and a low-affinity system involved in osmoregulation. *J Bacteriol* **174**: 2702-
948 2710.
949 Vaish, M., Price-Whelan, A., Reyes-Robles, T., Liu, J., Jereen, A., Christie, S., Alonzo, F., 3rd, Benson,
950 M.A., Torres, V.J., and Krulwich, T.A. (2018) Roles of *Staphylococcus aureus* Mnh1 and
951 Mnh2 Antiporters in Salt Tolerance, Alkali Tolerance, and Pathogenesis. *J Bacteriol* **200**.
952 van den Berg, J., Boersma, A.J., and Poolman, B. (2017) Microorganisms maintain crowding
953 homeostasis. *Nat Rev Microbiol* **15**: 309-318.
954 Vijaranakul, U., Nadakavukaren, M.J., de Jonge, B.L., Wilkinson, B.J., and Jayaswal, R.K. (1995)
955 Increased cell size and shortened peptidoglycan interpeptide bridge of NaCl-stressed
956 *Staphylococcus aureus* and their reversal by glycine betaine. *J Bacteriol* **177**: 5116-5121.
957 Vijaranakul, U., Xiong, A., Lockwood, K., and Jayaswal, R.K. (1998) Cloning and nucleotide
958 sequencing of a *Staphylococcus aureus* gene encoding a branched-chain-amino-acid
959 transporter. *Appl Environ Microbiol* **64**: 763-767.
960 Vollmer, W., Blanot, D., and de Pedro, M.A. (2008) Peptidoglycan structure and architecture. *FEMS*
961 *Microbiol Rev* **32**: 149-167.

962 Wengender, P.A., and Miller, K.J. (1995) Identification of a PutP proline permease gene homolog
963 from *Staphylococcus aureus* by expression cloning of the high-affinity proline transport
964 system in Escherichia coli. *Appl Environ Microbiol* **61**: 252-259.
965 Wertheim, H.F., Melles, D.C., Vos, M.C., van Leeuwen, W., van Belkum, A., Verbrugh, H.A., and
966 Nouwen, J.L. (2005) The role of nasal carriage in *Staphylococcus aureus* infections. *Lancet*
967 *Infect Dis* **5**: 751-762.
968 Wetzel, K.J., Bjorge, D., and Schwan, W.R. (2011) Mutational and transcriptional analyses of the
969 *Staphylococcus aureus* low-affinity proline transporter OpuD during *in vitro* growth and
970 infection of murine tissues. *FEMS Immunol Med Microbiol* **61**: 346-355.
971 Whatmore, A.M., and Reed, R.H. (1990) Determination of turgor pressure in Bacillus subtilis: a
972 possible role for K+ in turgor regulation. *J Gen Microbiol* **136**: 2521-2526.
973 Wood, J.M. (2011) Bacterial osmoregulation: a paradigm for the study of cellular homeostasis.
974 *Annu Rev Microbiol* **65**: 215-238.
975 Wyke, A.W. (1984) Isolation of five penicillin-binding proteins from *Staphylococcus aureus*. *FEMS*
976 *Microbiology Letters* **22**: 133-138.
977 Yao, J., Zhong, J., Fang, Y., Geisinger, E., Novick, R.P., and Lambowitz, A.M. (2006) Use of
978 targetrons to disrupt essential and nonessential genes in *Staphylococcus aureus* reveals
979 temperature sensitivity of Ll.LtrB group II intron splicing. *RNA* **12**: 1271-1281.
980 Zeden, M.S., Schuster, C.F., Bowman, L., Zhong, Q., Williams, H.D., and Gründling, A. (2018) Cyclic
981 di-adenosine monophosphate (c-di-AMP) is required for osmotic regulation in
982 *Staphylococcus aureus* but dispensable for viability in anaerobic conditions. *J Biol Chem*
983 **293**: 3180-3200.
984

985

986 **Figure legends**

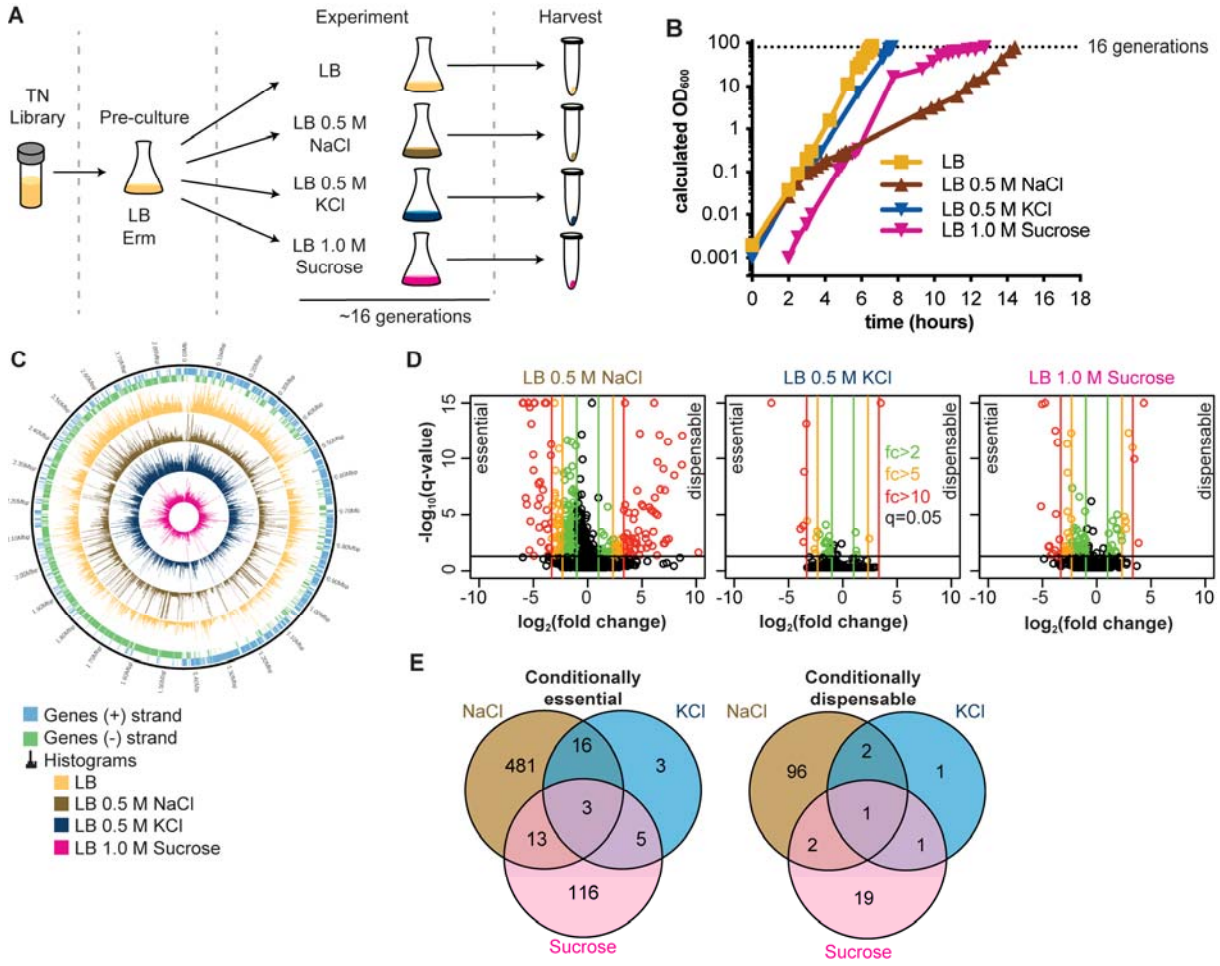

987
988

989 **Fig. 1. Different sets of genes are conditionally essential for the growth of *S. aureus* under NaCl,**

990 **KCl or sucrose stress conditions.**

991 A. Workflow of the TN-seq experiment. A TN-seq library was pre-cultured and then used to

992 inoculate LB, LB containing 0.5 M NaCl, 0.5 M KCl or 1 M sucrose. Cells were kept in exponential

993 phase for 16 generations, harvested and transposon insertion sites determined by high

994 throughput sequencing.

995 B. Growth curves. For the TN-seq experiment (n=1), the growth of an *S. aureus* library cultured in

996 LB, LB 0.5M NaCl, LB 0.5 M KCl or LB 1.0 M sucrose medium was followed by taking OD_{600}

997 measurements at timed intervals. The cultures were back-diluted once when they reached an

998 OD_{600} of approximately 0.3. The plotted OD_{600} values were calculated by multiplying the measured
999 OD_{600} with the dilution factor. The dotted line indicates the 16 generation cut-off at which cultures
1000 were harvested.

1001 C. Circular plot showing the transposon insertion density along the *S. aureus* genome under
1002 different osmotic stress conditions. The two outer rings depict genes located on the (+) or (-)
1003 strand in *S. aureus* strain USA300 FPR3757. The inner four rings show the histograms of
1004 transposon insertions on a per gene basis after growth of the library in LB (orange), 0.5 M NaCl
1005 (brown), 0.5 M KCl (blue) and 1 M sucrose (pink) medium for 16 generations.

1006 D. Volcano plots of conditionally essential and dispensable genes following growth of *S. aureus* in
1007 0.5 M NaCl, 0.5 M KCl or 1 M sucrose medium and compared to LB conditions. q-values represent
1008 Benjamini-Hochberg corrected p-values, and $\log_2$ (fold changes) indicate essential genes (negative
1009 values) or dispensable genes (positive values). The black horizontal line indicates a q-value of 0.05,
1010 which was deemed the significance level. Vertical lines indicate 2- (green), 5- (orange) or 10- (red)
1011 fold changes in either direction. Each dot represents one gene and coloring follows the fold-
1012 change scheme whenever the q-value threshold was met. Very small q-values were truncated to
1013 fit onto the graph. The TN-seq experiments were conducted once (n=1).

1014 E. Venn diagrams showing overlaps of conditionally essential and dispensable genes during
1015 prolonged NaCl, KCl or sucrose stress. Genes with a 2-fold decrease (essential genes) or a 2-fold
1016 increase (dispensable genes) in transposon insertions under each stress condition compared to the
1017 LB condition and a q-value of ≤0.05 were determined and the overlap between these gene lists
1018 displayed in Venn diagrams.

1019

1020

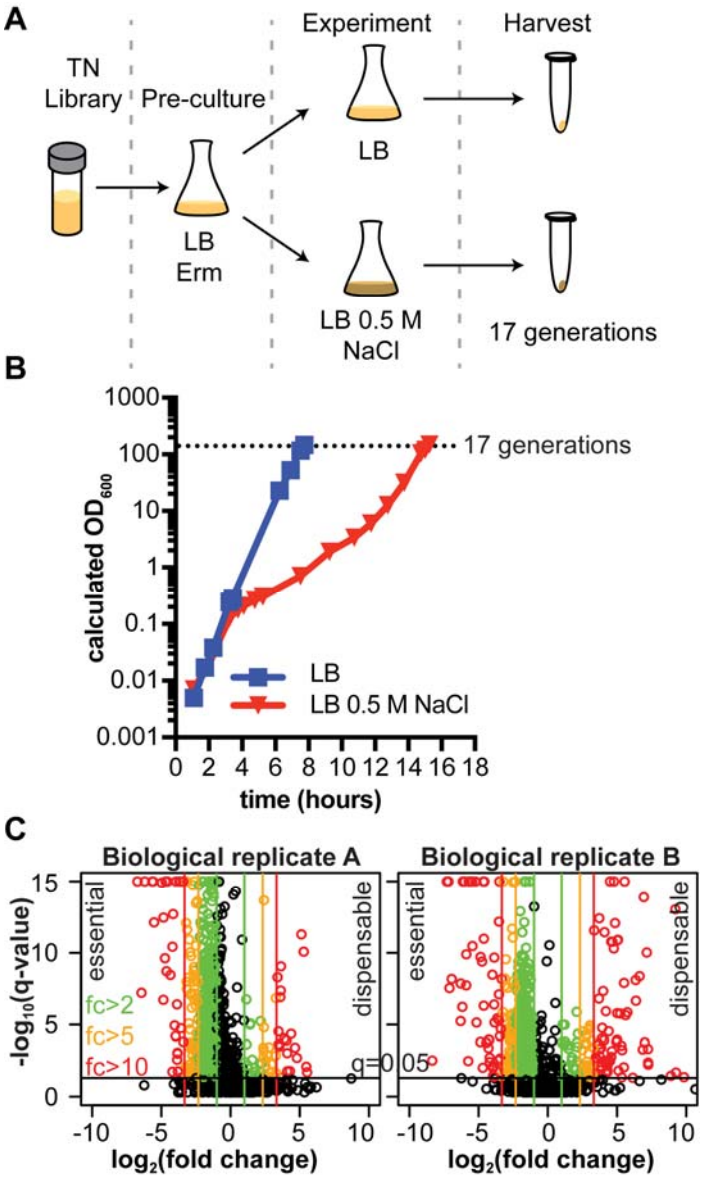

1021

1022 **Fig. 2. TN-Seq screen reveals essential and dispensable genes during prolonged NaCl stress in *S.***
1023 ***aureus*.**

1024 A. Workflow of TN-seq experiments. A saturated transposon library was pre-cultured for one hour,

1025 then used to inoculate LB medium containing either normal levels (0.086 M) or 0.5 M of NaCl.

1026 After 17 generations, cells were harvested, and transposon insertion sites determined by high

1027 throughput sequencing.

1028 B. Growth curve. Growth of the *S. aureus* library culture in LB and LB 0.5 M medium was followed

1029 by determining OD_{600} readings. Dotted line indicates the 17 generation threshold. Cultures were

1030 back-diluted once when they reached an OD of approximately 0.3 and the optical densities shown
1031 are calculated from measured ODs time dilution factor. Culture from replicate B (n=1) is shown
1032 and a similar growth profile was seen for replicate A.
1033 C. Volcano plots of essential and dispensable genes in NaCl conditions compared to LB. Negative
1034 $\log_2$ fold-changes indicate essential and positive $\log_2$ fold-changes dispensable genes. q-value
1035 stands for Benjamini-Hochberg false discovery rate. Black horizontal line indicates q-value of 0.05
1036 (cut-off) and red, orange and green vertical lines 10-, 5- and 2-fold differences in either direction.
1037 Colored circles indicate genes for which a significant change in the number of transposon
1038 insertions was observed above q-value cutoff and follow the same color code as the vertical lines.
1039 Very small q-values were truncated to fit onto the graph. Data from replicate A are shown in the
1040 left panel and from replicate B in the right panel (n=1 for each plot).

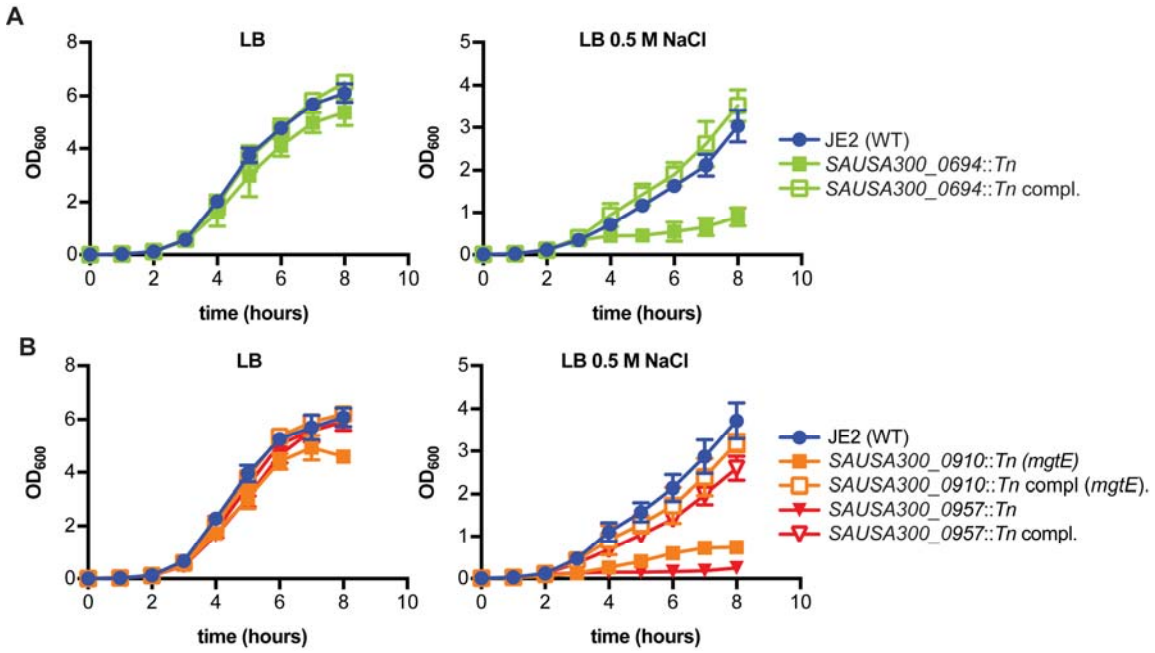

1041

1042 **Fig. 3. Growth curves and complementation analysis of *S. aureus* strains with transposon**

1043 **insertions in salt essential genes.**

1044 A-B. *S. aureus* strains JE2 (WT), *SAUSA300_0694::Tn* mutant with empty plasmid and

1045 complementation strain (A) or JE2 (WT), *SAUSA300_0910* (*mgtE*), *SAUSA300_0957::Tn* with empty

1046 plasmid (B) and respective complementation strains were grown in LB (left panels) or LB 0.5 M

1047 NaCl medium (right panels) supplemented with 100 ng/ml Atet and OD_{600} readings determined at

1048 timed intervals. Growth curves were performed in triplicates (n=3) and means and SDs of OD_{600}

1049 readings were plotted.

1050

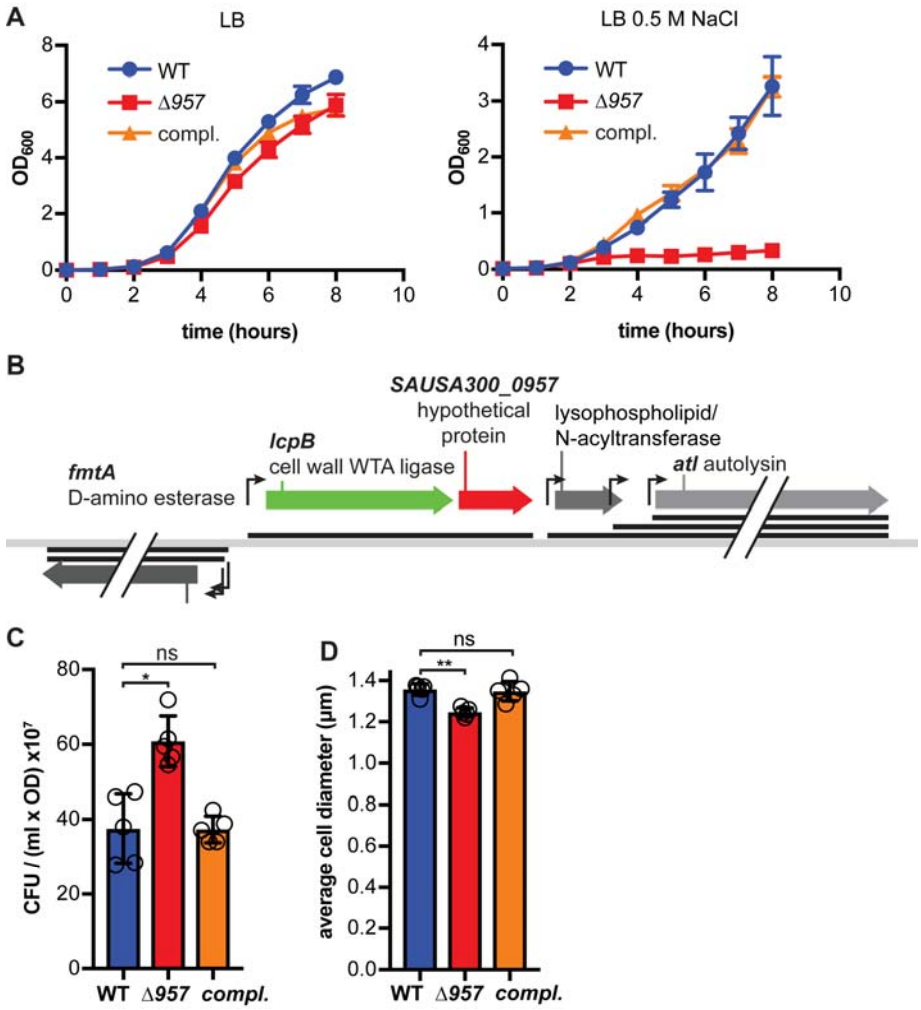

Fig. 4. Gene *SAUSA300_0957* is located in a genomic region with cell envelope genes and its deletion leads to salt sensitivity and other phenotypic changes.

A. Growth curves. *S. aureus* strains LAC* piTET (WT), LAC*Δ*957* piTET (Δ*957*) and the complementation strain LAC*Δ*957* piTET-*957* (compl.) were grown in LB or LB containing 0.5 M NaCl medium and 100 ng/ml Atet. The growth was monitored by determining OD_{600} readings the means and SDs from three independent experiments were plotted.

B. Schematic of the *S. aureus* USA300 FPR3757 chromosomal region with gene *SAUSA300_0957* (gene *957*). Putative promoters are shown as angled arrows (adapted from (Mäder *et al.*, 2016)) and black bars indicate the corresponding transcripts.

1062 C. Determination of CFU/OD ratios. OD_{600} values as well as CFU/ml were determined for overnight
1063 cultures of the *S. aureus* strains described in panel B and the means and SDs of the CFU per ml
1064 OD_{600} of 1 from five independent experiments were plotted.
1065 D. Cell size measurements. The cell walls of the *S. aureus* strains described in panel B were stained
1066 with fluorescently labelled vancomycin and the cells subsequently observed under a microscope.
1067 The diameters of 200 cells were measured and the means calculated. This average of the means
1068 and SDs from five independent experiments were plotted.
1069 For statistical analysis, a Kruskal-Wallis one-way ANOVA test was performed followed by a Dunn's
1070 post-hoc test to determine p-values. Asterisks (*) indicate $p \leq 0.05$ and two asterisks (**) $p \leq 0.01$
1071 and ns=not significant.
1072

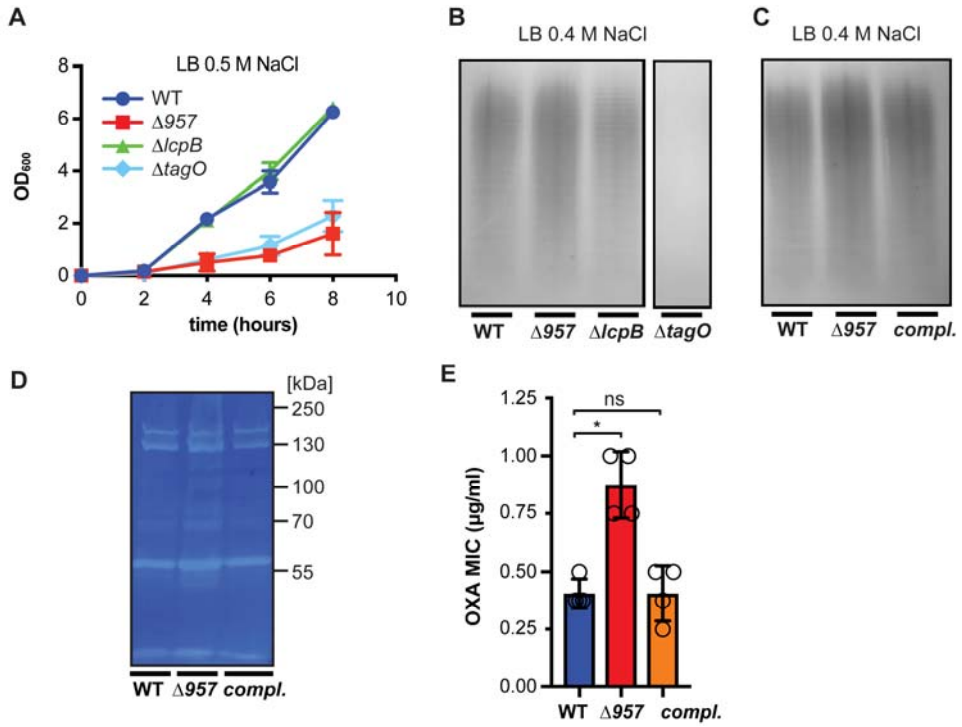

1073

1074 **Fig. 5. Inactivation of *gene 957* does not significantly alter WTA levels or autolysis but leads to**

1075 **changes in oxacillin resistance.**

1076 A. Growth curves. *S. aureus* strains LAC* (WT), LAC*Δ*957* (Δ*957*), LAC*Δ*lcpB*, (Δ*957*), and

1077 LAC*Δ*tagO* (Δ*tagO*) were grown in LB 0.5 M NaCl medium and OD_{600} readings determined at

1078 timed intervals. The means and SDs from three biological replicates were plotted.

1079 B. Detection of WTA on silver stained gels. WTA was isolated from *S. aureus* strains described in

1080 panel A following growth in LB 0.4 M NaCl medium. The WTA was separated by electrophoresis

1081 and visualized by silver stain. The experiment was performed three times and one representative

1082 gel image is shown.

1083 C. Detection of WTA on silver stained gels. Same as panel B but using the strains LAC* piTET (WT),

1084 LAC*Δ*957* piTET (Δ*957*), and the complementation strain LAC*Δ*957* piTET-*957* (compl.) grown in

1085 LB 0.4 M NaCl medium also containing 100 ng/ml Atet.

1086 D. Zymogram gel. Cell extracts prepared from *S. aureus* strains described in panel C were

1087 separated on a gel containing heat killed *Micrococcus luteus* cells. Autolysins were renatured and

1088 the zones of lysis visualized by methylene blue staining. The experiment was performed twice and

1089 one experiment is shown.

1090 E. Determination of oxacillin MICs. Oxacillin MICs were determined for *S. aureus* strains described

1091 in panel C using Etest strips. The median and SDs from four biological replicates were plotted.

1092 For statistical analysis, a Kruskal-Wallis one-way ANOVA test was performed followed by a Dunn's

1093 post-hoc test to determine p-values. Asterisks (*) indicate $p \leq 0.05$ and ns=not significant.

1094

1095

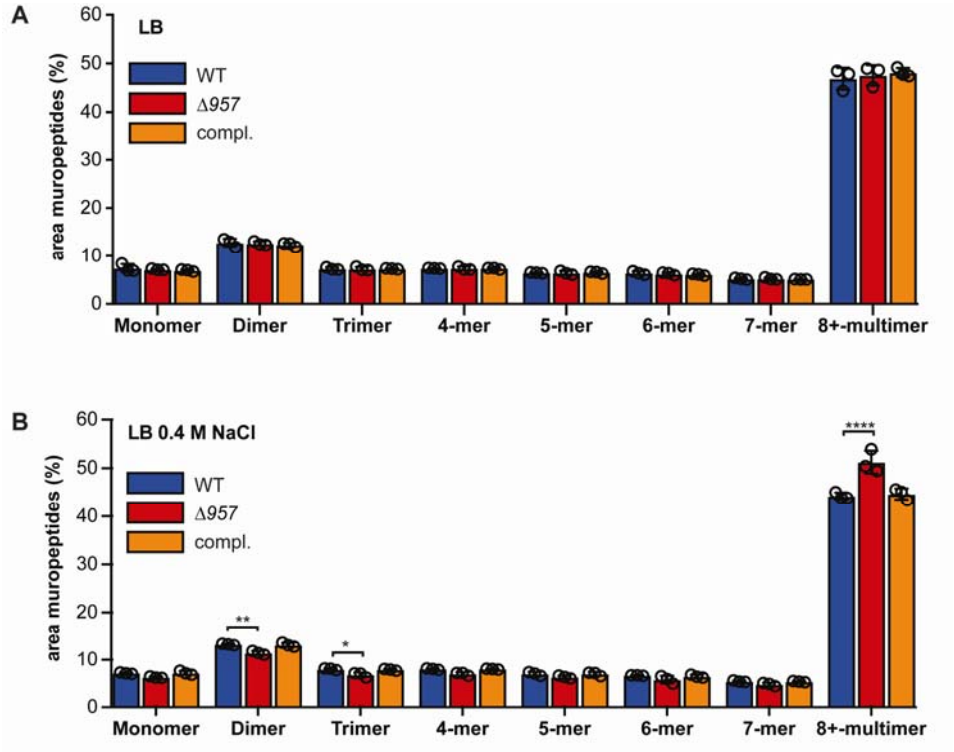

1096 **Fig. 6. Inactivation of *gene 957* leads to an increase in peptidoglycan crosslinking.**

1097 A-B. Muropeptide quantification. *S. aureus* strains LAC* piTET (WT), LAC*Δ*957* piTET (Δ*957*), and
1098 the complementation strain LAC*Δ*957* piTET-*957* (compl.) were grown in either LB (A) or LB 0.4 M
1099 NaCl (B) containing 100 ng/ml Atet. After reaching late-exponential phase, the peptidoglycan was
1100 isolated, digested and the muropeptides separated by HPLC. The areas under the peaks from the
1101 chromatograms (representative chromatograms are shown in Supplementary Fig. S8) were
1102 quantified for each mono-, di- or multimer. Bars represent means, and error bars standard
1103 deviations from three independent experiments. For statistical analyses, two-way ANOVAs were
1104 performed, followed by Dunnett's post-hoc tests using the WT as a comparison. The differences in
1105 (A) were not significant. For (B), one asterisk (*) indicates $p \leq 0.05$, two asterisks (**) $p \leq 0.01$ and
1106 four asterisks (****) $p \leq 0.0001$.

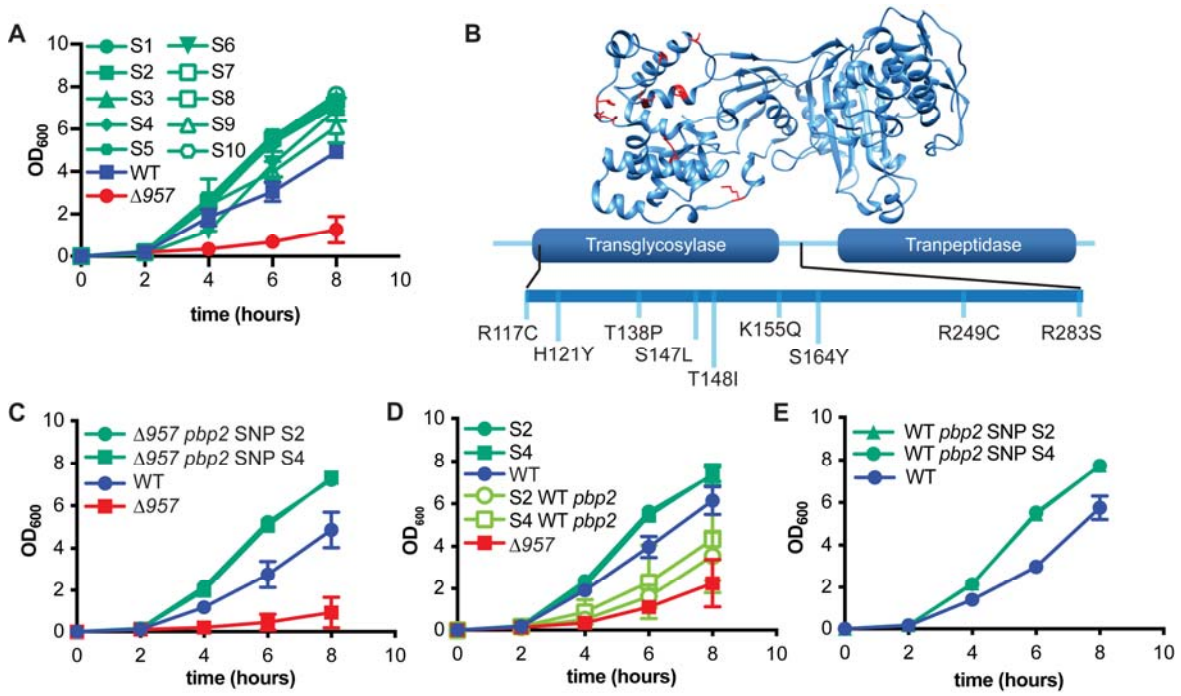

1107

1108 **Fig. 7. The growth and peptidoglycan defect observed for the *957* mutant can be rescued by**

1109 **compensatory mutations in *pbp2*.**

1110 A. Growth curves. *S. aureus* strains LAC* (WT), LAC*Δ*957* (Δ*957*) and the LAC*Δ*957* suppressors

1111 S1-10 (S1 to 10) were grown in LB 0.5 M NaCl medium, OD_{600} readings determined and the means

1112 and SDs of four biological replicates plotted.

1113 B. Schematic of Pbp2 with amino acid substitutions identified. Top: Structure of the *S. aureus*

1114 penicillin binding protein Pbp2 (PDB: 3DWK, (Lovering *et al.*, 2008)) with amino acids that are

1115 altered in the obtained suppressor strains shown in red. Bottom: Schematic of the Pbp2 enzyme

1116 with the transglycosylase and transpeptidase domains as well as the observed amino acid changes

1117 in the transglycosylase domain indicated.

1118 C. Growth curves using *957* mutant strains containing *pbp2* alleles from suppressors S2 and S4.

1119 Growth curves were performed in LB 0.5 M NaCl medium and plotted as described in panel A but

1120 using *S. aureus* strains LAC* *1332*::Tn (WT), LAC*Δ*957* *1332*::Tn (Δ*957*), LAC*Δ*957* *1332*::Tn *pbp2*

1121 SNP S2 (Δ*957* *pbp2* SNP S2), LAC*Δ*957* suppressor S4 *1332*::Tn (Δ*957* *pbp2* SNP S4).

1122 D. Growth curves using *957* suppressors with their *pbp2* gene repaired to WT. Growth curves were

1123 performed in LB 0.5 M NaCl medium and plotted as described in panel A but using *S. aureus*

1124 strains LAC* *1332*::Tn (WT), LAC*Δ*957* *1332*::Tn (Δ*957*), LAC*Δ*957* suppressor S2 *1332*::Tn (S2),

1125 LAC*Δ*957* suppressor S4 *1332*::Tn (S4), LAC*Δ*957* suppressor S2 *1332*::Tn repaired WT *pbp2* (S2

1126 WT *pbp2*), and LAC*Δ*957* suppressor S4 *1332*::Tn repaired WT *pbp2* (S4 WT *pbp2*).

1127 E. Growth curves using WT strains carrying *pbp2* SNPs. *S. aureus* strains LAC* *1332*::Tn (WT), LAC*

1128 *1332*::Tn *pbp2* SNP S2 (WT *pbp2* SNP S2) and LAC* *1332*::Tn *pbp2* SNP S4 (WT *pbp2* SNP S4) were

1129 grown in LB 0.5 M NaCl medium and OD_{600} readings determined and the means and SDs of three

1130 biological replicates plotted.

1131

1132

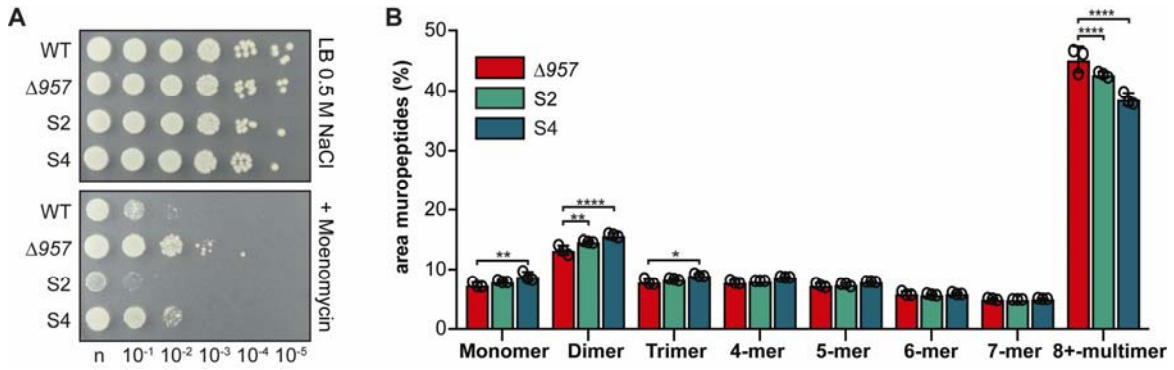

1133 **Fig. 8. The Δ*957* suppressor strains show decreased peptidoglycan crosslinking compared the**

1134 **Δ*957* mutant.**

1135 A. Bacterial growth on moenomycin supplemented agar plates. *S. aureus* strains LAC* (WT),

1136 LAC*Δ*957* (Δ*957*), LAC*Δ*957* Suppressor S2 (S2) and S4 LAC*Δ*957* Suppressor S4 (S4) were grown

1137 to exponential phase, normalized to an OD_{600} of 0.1 and plated either neat (n) or in 10-fold

1138 dilutions onto LB agar containing 0.5 M NaCl without (top) or with (bottom) moenomycin. Shown

1139 is one representative image of three biological replicates.

1140 B. Muropeptide analysis. *S. aureus* strains LAC*Δ*957* (Δ*957*), LAC*Δ*957* Suppressor S2 (S2) and S4

1141 LAC*Δ*957* Suppressor S4 (S4) were grown in 0.4 M NaCl LB medium and muropeptides quantified

1142 as described in Fig. 5. Representative chromatograms are shown in Supplementary Fig. S10D. The

1143 means and SDs from three biological replicates were plotted. For statistical analysis a two-way

1144 ANOVA and Dunnett's post-hoc test was performed. One asterisk (*) indicates $p \leq 0.05$, two

1145 asterisks (**) $p \leq 0.01$ and four asterisks (****) $p \leq 0.0001$.

1146